CORRELATION OF RADIO WAVE WITH PHOTOMETRIC LIGHT FOR REPRESENTATION OF RADIO LOSS USING TRANSPARENT FILM AND ITS IMPLEMENTATION USING MATLAB

by

Ashutosh Yadav, B.S.

A thesis submitted to the Graduate Council of
Texas State University in partial fulfillment
of the requirements for the degree of
Master of Science
with a Major in Engineering
December 2018

Committee Members:

George Koutitas, Chair

William Stapleton

Semih Aslan

FAIR USE AND AUTHOR'S PERMISSION STATEMENT

Fair Use

Duplication Permission

ACKNOWLEDGEMENTS

First of all, I would like to thank my supervisor Dr. George Koutitas for his support and guidance during the past two years. I feel grateful to have worked under such an inspiring researcher who has given me this opportunity to learn from his wisdom. I would also like to thank my committee members Dr.William Stapleton and Dr.Semih Aslan for their many positive and fruitful feedback which have directed a big part in my thesis. I am really grateful for their generous support for the successful completion of my thesis.

Finally, I would like to thank my family and friends for their motivation and encouragement all these years of my studies. My mother and father has supported me during the difficult times and inspired me throughout my research.

TABLE OF CONTENTS

LIST OF TABLES

Table **Page**

LIST OF FIGURES

Figure **Page**

ABSTRACT

The demand for wireless communication has significantly grown in recent years. The number of communicating devices is increasing with the development of new RF circuits design and integrated circuits which makes it possible to reach new innovations in wireless technologies. A growing demand by the users makes it difficult for proper planning of radio communication processes in indoor environmental conditions. In in-building communication, coverage regions are reduced by frequency, multipath, diffraction, scattering, reflection and shadow fading. Indoor systems require large numbers of base stations depending upon the diverse arrangement which inevitably increases the level of interference from the neighboring cell. Also, the planning system requires building vector data, propagation model parameters, obstacle information, and antenna models which makes planning and optimization of an indoor system an extremely complex and tedious process. To account all these problems, a proper and simple propagation model is needed to predict the accurate path loss between the transmitter and receiver in different indoor conditions. This purpose can be achieved by implementing the propagation model in real-world situations using Augmented Reality (AR). AR has been in use for many years in applications like smartphones, video games, Military, Navigation and so on. This thesis explores on developing a semi-deterministic propagation model and a way to implement this model using AR. The research focuses on evolving a propagation model that is centered on the perception of the radio wave by the human eye. The behavior of the human eye with visible light is understood and

accordingly, the investigated behavior is correlated with the radio wave. The correlation helps to envision radio wave by human eye as a light wave. AR facilitates visualization of an indoor surrounding with radio wave with its coverage distinguished by different transparent films to visualize the coverage of different antennas. The result of this association provides a new technique of designing propagation channels in an indoor wireless environment using free space loss and wall loss. The investigation of this research helps to change the way people interact with the radio wave environment in their daily lives with the detailed and simplified planning process.

1. INTRODUCTION

1.1 General Overview

The electromagnetic spectrum consists of all the frequencies corresponding to the electromagnetic radiation. The spectrum contains radio waves, microwaves, gamma ray, visible light and each set of frequencies have their own characteristics. Wireless communication is a field that encompasses the transfer of information using radio waves ranging from 3 KHz to 300 GHz. There are a wide range of radio communication systems like High Frequency (HF), Very high (VHF,30-300 MHz), Ultra high (UHF,300 MHz-3 GHz), Super high (3-30 GHz) and Extremely high used for satellite (30-300 GHz). There are many wireless communication systems that permit sharing of information using these frequency choices like infrared communication, microwave communication, Wi-Fi technology (WLAN), mobile communication system and Bluetooth Technology (personal Communication system). These communication systems range from a few meters to hundreds of kilometers depending on the necessity of the system. The mobile communication system can cover a wide area due to the need to provide seamless coverage for a large number of mobile users in the outdoor environment. The mobile users are always moving from one place to another requiring a wide coverage radius of the system to satisfy user experience. Cellular technology is necessary to have a reliable connection for voice calls in outdoor and indoor scenarios. On the other hand, indoor communication systems like Wi-Fi are essential for customers that reside in buildings for reliable access to the internet network. Wi-Fi is suitable for distances of a few meters to few kilometers depending on the frequency and power used. Other communication

systems like Bluetooth, infrared and other personal systems are used for communication for few meters. These systems are used for short-range communication processes which utilize less bandwidth for sharing information. All these technologies are abundantly available due to the increase in a number of devices. The increase in the users' equipment has increased the demand for better accessibility of the network. The network operators are responsible for providing the best service to the customer but the increase in the percentage of the radio wave in the environment has made planning and optimizing networks extremely difficult. This research paper focuses on providing a solution to indoor wireless communication systems.

Various channels are used for sharing information in uplink and downlink process through radio wave communication. The channel number distinguishes the technology and service needed for each specific type of communication process. Channels must be properly spaced to reduce the possibility of interference. Likewise, man-made objects in indoor scenarios are responsible for scattering through small irregularities, diffraction by sharp edges, reflection by plane surfaces, transmission through materials like walls and floors, and fading of signal due to multi-path. This phenomenon changes characteristics of a radio wave which gradually increases the rate of error in the message signal. All these factors are needed to be addressed for developing the finest wireless communication method for the user. Therefore, there is a need for proper modeling of radio channel to achieve the key performance indicator of the network. The modeling of radio channels can be done by predicting the characteristics like distance (LOS path loss), the number of objects intersected, delay due to multipath, bandwidth requirement like

narrowband or wideband, frequency, time variance, the direction of arrival and others. The propagation model is needed to determine the behavior of the radio channel which accordingly assists to predict the signal strength of a radio wave. The model design is a critical process as it should state the precise path loss of the radio signal. This thesis emphasize on precise modeling of a radio channel in an indoor wireless environment. [1]

1.2 Problem Statement

The planning of an indoor wireless network is based on two factors: Cost analysis and Technical attribute. Firstly, the cost of planning a network is analyzed and consequently, a propagation model is implemented in the technical phase. The coverage planning should consider the budget before estimating the parameters and services required to provide the planned requirements. Customer requirements include seamless coverage planning, high data throughput, lower interference and a high penetration of signal all of which can only be fulfilled with an increase in station or antennas and bandwidth. This will increase the need for higher frequency and higher transmission bandwidth making radio planning a complex process. [1]

Technically, it is necessary to implement a propagation model for determining the propagation properties of an indoor wireless system. The propagation characteristics are important for proper coverage planning of an antenna requirement in an in-building environment. The propagation model requires prediction of multipath of a signal, fading properties, and cell radius. The radio wave propagation is required for a macro, micro and picocell cell coverage due to the availability of users in environments. The proper

planning and modeling of radio channel required for these cells can be achieved through planning steps. The planning is done with the help of tools that includes all the necessary features required for planning procedure. A planning tool requires a detailed digital map of the environment in the first phase that includes all the indoor details like walls, windows, table, chairs, and of floors. Secondly, there is a need for propagation model that is based on theoretical assumptions, empirical calculations and deterministic approach or combination of these models. The propagation model calculates the path loss between the transmitter and receiver using the parameters of that model. The location of antennas is determined using the path loss prediction using the simulation tool. Path loss prediction helps to evaluate the antenna requirement based on signal strength.

Propagation mechanisms are based on the design criteria of a model. The theoretical and deterministic models are based on assumption, and their validity holds for the set-up although various parameters can be altered in the process. Empirical models are built on experiments on the field, but the behavior of radio waves illustrate a mixture of different propagation models ranging from macro, micro, and pico-cell prediction. The planning of a system is complex and irregular. There is a need for appropriate planning method that can offer a straightforward planning process and precise prediction result. The user should not depend on network providers to experience, plan, analyze, or predict the radio wave signal. The signal strength of radio waves can be visualized in AR devices, and the user can design the indoor Wi-Fi systems based on the observed radio characteristics. A user's position can be adjusted to overcome the weak signal strength caused by obstacles

between the modem and the user. Alternatively, the obstacle can be moved to a new location based on the users' intent. This research will concentrate on developing a way to simplify the planning process with the help of AR application based on a semi-deterministic propagation model for precise measurements. The Propagation is accomplished by correlating concept of light and radio wave.

The idea is to convert the radio wave propagation loss into light wave transparency values as perceived by human eyes for predicting the path loss. The association of two phenomena will help to observe the radio wave with the naked human eye by exploiting augmented reality applications. This new propagation model uses an insight of an eye which will develop a new platform for designing a path loss model. The theoretical attributes of this model will broaden the knowledge of defining any propagation prototype depending on the perception of light by human eyes for every indoor situation.

1.3 Literature Review

It is important to characterize and design a channel to understand the propagation mechanisms of a radio wave in an indoor wireless system. A propagation model provides a precise estimation of the path covered by a radio wave. It is a tedious procedure to collect the data from every part of an indoor environment, which consequently increases the planning cost. The existing propagation models are theoretical, empirical and deterministic. Theoretical models are based on verified mathematical laws and concepts. The determined equation based on these laws predicts the path loss in multiple environments. The advantage of theoretical modeling is it requires less input data and

provides a desirable result in multiple indoor environment. The Diffraction screens model is based on theoretical Walfisch-Bertoni [2] model, which estimates the diffraction of rows or blocks of the building. This model views the building as the diffraction screens and the propagation loss is estimated based on the multiple forward diffraction caused by the screen on the process [2].It makes a theoretical assumption that provides a power dependence of the signal with numerical calculations [2].The Free space path loss model is another theoretical model that estimates the received power dependence with the distance under free space environment [3]. Although, the mathematical calculations are primitive in nature, the robustness of the estimated calculation is complex. The predicted assumptions based on theory does not guarantee its validity. Theoretical models provide a basis to design an empirical model based on mathematical estimations and consequently, helps in designing the experimental environment to collect data.

The empirical or statistical propagation [4] models are based on stochastic variables that does not include site–specific data. These models rely on the equations derived from extensive field measurements. The empirical models are used for characterization of the propagation mechanisms like multipath fading, path loss and shadowing. These models estimate the quality requirement of the service [5].Some of the examples are narrow band empirical models, like one slope model [6], multi-wall model [1], and linear attenuation model [1]. Empirical wide-band models are used for small-scale characterization of the propagation mechanisms based on delay spread ,power delay, delay spread, doppler spread, and coherence time. The simplest propagation model used in indoor wireless systems is COST 231 one-slope model, which has a linear dependence on the path loss

calculated at reference of 1 meter and the logarithmic distance [6].This model generally estimates the power decay of the transmitted radiation corresponding to the distance between transmitter and receiver and does not account for other losses. Correspondingly, the log-distance model depends on the logarithmic distance with path loss exponent. The path loss exponent is the factor of the type of material used in the building [7]. This model does not estimate the clutter variations on different transmitter and receiver locations. The Log-normal shadowing model considers all the variations of the environmental clutters due to the shadowing effects having the same Transmitter-Receiver (T-R) separation on different locations [7]. Motley and Keenan [8] developed a sophisticated version of the log-distance model, which accounts all the individual penetration loss of walls and floors with respect to the material and their thickness. The model estimates the linear dependence of the penetration loss, but research using ray-tracing algorithm suggested non-linear variation of penetration loss [9]. Thus, the COST 231 multi-wall model is developed to account the free space path loss , losses due to walls and non-linear variation of the penetrated floors by adding an empirical factor on the model design [1]. The loss of wall is predicted with the help of a constant developed by the linear regression technique [1]. The total wall loss is determined by adding the loss of each wall in T-R separation. Although, this model does not include multiple penetrated floors, it precisely estimates the multiple effects of the walls. The Wide-band empirical model like log-Normal fading model [7], Ricean distribution [7], Suzuki model [10], Weibull model [11] based on small-scale characterization of fading and respectively, the Two-ray Rayleigh fading model [7], Saleh and Valenzuela model [12], discrete time model [13] for delay spread. Propagation mechanisms like reflection, refraction,

scattering and diffraction leads to time dispersion and fading at random places. All these wideband empirical models provides an insight into various channel characterization losses, but the proper prediction results have not been accounted due to the site-specific features of the indoor environment systems. These effects have been anticipated using the deterministic approach due to its site-specific characteristics. The deterministic propagation models are based on wave theory and require precise collection of site data that includes number of floors, walls, windows, building materials, obstacles and so on. These models are identified using geometric optics (GO) and finite difference time domain. The geometrical optics technique is most widely used due to its efficiency with computer-based simulations. Ray tracing is one of the widely used geometrical techniques used to predict the rays radiating from antenna in an indoor environment [1]. Ray tracing using uniform theory of diffraction is a deterministic approach to account the pattern of the signal being reflected and diffracted. Uniform theory of diffraction is an extended form of geometric optics, which includes diffracted rays unlike direct, reflected and refracted rays considered in GO [14] . This method accounts for all the rays that have undergone reflection and diffraction between T-R separation [14]. Consequently, the scattering characteristic of the radio wave propagation is estimated by the Two-ray model [15], using the properties of reflection and refraction. The ray predicts the direct path and reflected path, and consequently, the transmission and reflection features are analyzed using permittivity of the obstacle. GO techniques provide desirable results for simple indoor conditions but it fails to satisfy the scattering characteristics in a complex environment. The Finite Difference Time Domain (FDTD) provides a relatively simple alternative to estimate the scattering mechanism of a wave. It accurately calculates all the

points on the map to predict the real coverage area. A hybrid combination of GO and FDTD is alternatively used to reduce the computation time and memory required by FDTD [4].

Every model has its advantages and disadvantages due to the wide range of factors affecting propagation characteristics. The hybrid combination of the empirical method and the deterministic model have been examined due to the need to account all the losses. There has been extensive research done on the hybrid models where empirical parameters are utilized to design the model, and the deterministic approach are used to physically simulate this model. The most widely use of this approach is COST-231 model. The COST-231 model is derived from the Okumara-HATA model, a widely used outdoor propagation model, which has demanded for its extension in an indoor wireless system for higher frequency [1]. Also, a semi-deterministic model has been developed using an empirical aspects, like prediction error and root mean square error of COST-231 Walfisch-Ikegami propagation model and deterministic characteristics are implemented using image method [16]. The hybrid combination provides a close approximation of the propagation characteristics alongside the attenuation caused by internal walls, corners, unsmooth surfaces and the distance between transmitter and receiver location. Such a semi-deterministic approach provided an improvement over the individual empirical and deterministic methods for path loss prediction, but there are many uncertain and unidentified factors, which affect the behavior of radio waves. These factors have distinctive impacts on the performance depending upon the in-building environment, like building design, materials used, number of human interactions, and man-made obstacles,

which changes on a daily basis. Furthermore, deployment of such models requires computer-based tools like iBwave, Atoll, Asset, Auto-CAD, MapInfo, Global Mapper and so on to design the network. The proper planning of an indoor network requires large a number of computer-based devices, testing equipment, software, digital-map, and human resources. The optimization process may require detailed parameters used in the planning process with some additional testing requirements for improving the network. Such complex designing, and planning makes an indoor system an expensive task for an operator. [1]

While the propagation of radio wave is understood and predictable, using this to improve and optimize wireless channels is difficult. There is a need for a device which simplifies this process and makes it easier for operators and consumers. This thesis research focuses on creating a process of low-cost and precise designing of a model for simple planning and optimization. The research would remove the complexity of planning and of indoor systems by visualizing the radio condition. This accessibility of radio wave characteristics would be made possible using augmented reality methods. The research would develop a model which will include empirical parameters like path loss and loss due to walls. The empirical model would be simulated using augmented reality applications which would allow us to interconnect with an indoor environment to envision the path loss of radio wave by depicting transparent film. This would remove the hectic planning process, time and cost involved in planning and optimizing the network. The need for such tools would not be necessary as we can picture the propagation feature on devices and make the necessary decision based on the surveillance with a naked eye.

Shaw [17] provided a conceptual understanding of Friis Equation using the optical radiometry and scalar diffraction. The proposed derivation removed the complexity of understanding the free space model with antenna impedance. It shows the equation dependence with the squared wavelength and difference of throughput in different antennas. In this thesis paper, the implementation of transparency film is achieved through the concept of relating Friis equation and photometry. Shaw's concept of relating two electromagnetic concepts provide a conceptual basis for designing a free space model with photometric luminance in this research. The implementation of the model can be accomplished using Augmented reality. A large number of research are focusing on a solution to visualize radio waves coverage in an indoor environment. Radio waves display [18] is a technique that consists of 20 by 20 radio sensors to provide a real-world visualization of radio waves. The field strength sensors are converted to visible light to picture the color of the wave passing through it. The technique only provides color depiction of different waves and does not account any human interaction with the real-world waves. Steve Mann [19] developed a sequential wave imprinting machine in 1970s using AR of physical occurrences, also known as phenomenal AR. The technique made invisible sound and radio wave visible by imprinting signal oscillations on the retina or photographic film using persistence of exposure. The model was a giant oscilloscope using linear arrays and when waved through space, it visualizes the signal pattern on the same place as they are [19]. There are some researches on an improvised SWIM technique to make it more compact and wearable using two transistors per picture elements [20] and to understand the concepts of wavelength measurement in real time and space [21]. A research has developed a multi-mediated reality which combines

features from all the reality (All R) that allows direct interaction with the real-world phenomenon with human actuators besides five senses. This approach helps to see radio waves and sound waves and their interaction with surrounding objects and each other [22]. Although all these research provides a background on making invisible waves to visualize, interpret and interact on a real-world scenario, not much imitation has been done on designing a propagation model using AR applications to predict the path loss in an indoor environment. Those research definitely provide an insight on how they can be utilized in future propagation channel modeling. Accordingly, this thesis provides an alternative AR based solution to interact with radio waves with semi-deterministic propagation modeling. The solution is based on the projection-based AR of radio wave transparency calculated using a propagation model and is discussed in section 1.4.

1.4 Augmented Reality

A computer-generated reality and graphics have widely grown since the implementation of augmented reality. Video games, cell phones, television and plenty of other innovation has demonstrated the use of simulated reality. Virtual reality creates a computer simulated circumstance with all the pre-defined objects and environment conditions. The reality is based on the designer's imagination, and the user has the ability to experience the application through virtual reality devices. Unlike, the virtual reality where the interaction of human is exclusive with the computer-generated world, augmented reality broadens the dimension of human interaction to real-world scenarios. Augment means enhancing or adding to something already existing. The augmented reality enhances the user experience by adding various computer-generated objects to the real world and

provides the flexibility of interacting with those objects. The objects projected in the real world have the ability to influence all the senses of a human being depending upon the circumstances. The user perceives the simulated objects as a part of a real-world environment and exploits their feature to communicate with real objects in the surrounding. The augmented reality has made it possible to see, hear, feel, smell and touch things which are beyond the limit of normal senses. The informative graphics and audio are widely used in many applications as the essential feature in augmented reality devices. The devices can look from a normal pair of glasses, a head-mounted display, finger sensitive display, contact lenses, optical projection system, Eye tap, spatial AR and many more [23-25]. The aspects of augmented reality are dependent on the application. Most of the augmented reality types can be categorized as marker-based augmented reality [26], marker-less augmented reality [27], projection-based augmented reality [28] and augmented reality based on superimposition [29]. The marker-based technique uses a camera and a marker code to recognize the objects from the environment. It provides a distinction of the surrounding things with less processing time [26]. Marker-less AR utilizes the global positioning system to provide the required database to the system. The GPS is accommodated with accelerometer, compass, gyroscope and many more in an embedded form to provide the precise data [27]. It is widely used in location centric application like finding restaurants, and business, direction mapping, and so on. The projection-based AR envisions the graphics using the light on to the real-world surface. The light is sensed with the human interaction with a touch or blink of an eye. The projected light on a surface is altered with human interaction and is distinguished by comparing with reference projected light [28]. The holographic display is the commonly

used application which can be illuminated in a three-dimensional view. The superimposed AR substitutes the real-world view of an object with a new or partial view of the same object [28]. The main basis of the technique is to recognize the object to be augmented and implement it on the practical scenario. The application of such AR are utilized by head-mounted displays such as HoloLens which uses optical system to superimpose computer-generated graphics on a crystal layer of a user's line of sight. Such AR are widely used in medicinal field like X-ray vision to observe the live ultrasound scan of the organs [29].

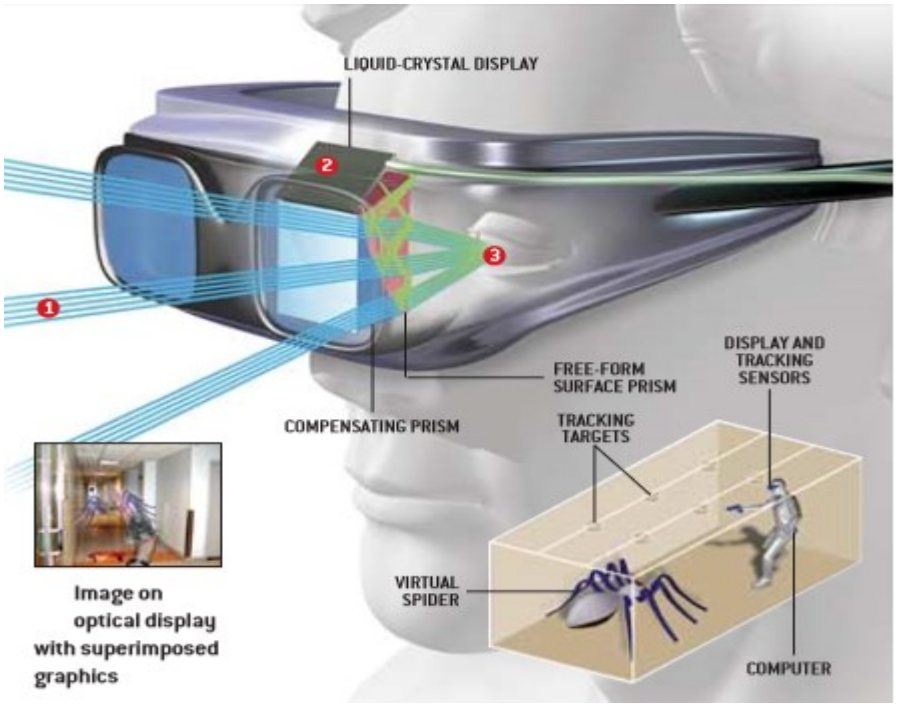

Figure 1.1 Virtual and real-world combination using Augmented reality[29]

This thesis research focuses on utilizing the application of AR to provide a much simpler and interactive radio wave condition. This research attempts to provide a simulated reality of the radio wave conditions in an indoor real-world environment. The path loss

prediction provides a basis to design a computer-generated reality of radio wave using the characteristics of transparent film. The film is designed to have transparency value depending upon the path loss predictions in a typical environment. The augmented reality adds up the transparent film element between a transmitter and receiver providing the virtual representation of radio wave. The AR devices use cameras and sensors to detect the surrounding environment and human interaction respectively. These cameras can be used to scan and collect element data of an indoor wireless environment [23]. The collected data is processed and interpreted using components like GPU, RAM, CPU, flash memory, Wi-Fi chip, GPS chips and many more. The interpreted data can be either envisioned on the mirrors of the AR devices or projected on the real-world surfaces like wall, tables, hands and many more. This research requires data to be projected on the mirrors of the devices for the visual effect of the film transparency on a real-world environment. The mirrors process the data from the incoming light into the camera and interpret the required data to be projected to the human eye with the help of reflection. The light enters the eye at a specific angle with specific intensity and color to produce an image on the eye's retina. This retinal image can be used to provide a virtual image of a film with path loss characteristic in the real environment. The path loss can be predicted with the use of the scanned indoor environment with elements like free space distance, intersected walls, doors, and windows, multipath and others. The path loss image and real-world image can be combined together to provide an augmented reality of the radio wave. The strength or the intensity of radio wave is the transparency of the path loss image mounted on a scanned indoor image to provide a virtual image

2. PROPAGATION ASPECTS IN RADIO WAVES

2.1 Wi-Fi Technology

The internet has become the integral parts of our lives in the 21st century with an increase in demand for sharing information in every business. The exchange of data from one user to another user is critical as everything is digitalized with respect to the communication. The internet is the interconnection of devices on a network that allows us to interact and share with everybody in this world. Unlike in the 1970s and 1980s where the internet was owned by United government, the information like emails, sharing photos, interactive live business meetings, live streaming, editing, playing online games, voice-call has become quite common with the commercialization [30] .Consequently, leading to decentralization of the internet for sharing, selling, exchanging goods and services within seconds[30] . Wi-Fi over the years has become the dominant LAN technology to provide the necessary internet access to the user since it uses unlicensed frequency band, unlike cellular technology. 'Wireless Fidelity' Wi-Fi refers to an over-the-air connection with a wireless client and a base between two wireless clients [30]. WLAN allows users to connect to the internet with the help of devices equipped with network interface card with the flexibility to move within the coverage area of access point ranging from 50-100m in comparison to wired LAN where the user must connect via cable. Wi-Fi is standardized by the Institute of Electrical and Electronics Engineers (IEEE) as Wireless Ethernet 802.11b for transmission of internet data protocol using radio waves. This technology provides much higher throughput than the dial-up connection and

cellular technology with the help of DSL, satellite, cable
modems. The technology is based on the OFDM (orthogonal frequency division multiplexing) radio standards which can transmit a large number of digital data through the radio waves. Wi-Fi is extensively suitable for high population density with much less coverage area and can accommodate large subscribers due to higher bandwidth compared to other technologies. Wi-Fi hotspot is planned in a
spot by spot environment required to provide reliable, high speed and fewer mobility services with unlicensed frequency as shown in figure 2.1. The internet has become the integral parts of our lives in the 21st century with an increase in demand for sharing information in every business. The exchange of data from one user to another user is critical as everything is digitalized with respect to the communication. The internet is the interconnection of devices on a network that allows us to interact and share with everybody in this world. Unlike in the 1970s and 1980s where the internet was owned by United government, the information like emails, sharing photos, interactive live business meetings, live streaming, editing, playing online games, voice-call has become quite common with the commercialization [30]. Consequently, leading to decentralization of the internet for sharing, selling, exchanging goods and services within seconds [30]. Wi-Fi over the years has become the dominant LAN technology to provide the necessary internet access to the user since it uses unlicensed frequency band, unlike cellular technology. 'Wireless Fidelity' Wi-Fi refers to an over-the-air connection with a wireless client and a base between two wireless clients [30]. WLAN allows users to connect to the internet with the help of devices equipped with network interface card with the flexibility to move within the coverage area of access point ranging from 50-100m in comparison to

wired LAN where the user must connect via cable. Wi-Fi is standardized by the Institute of Electrical and Electronics Engineers (IEEE) as Wireless Ethernet 802.11b for transmission of internet data protocol using radio waves. This technology provides much higher throughput than the dial-up connection and cellular technology with the help of DSL, satellite, cable modems. The technology is based on the OFDM (orthogonal frequency division multiplexing) radio standards which can transmit a large number of digital data through the radio waves. Wi-Fi is extensively suitable for high population density with much less coverage area and can accommodate large subscribers due to higher bandwidth compared to other technologies. Wi-Fi hotspot is planned in a spot by spot environment required to provide reliable, high speed and fewer mobility services with unlicensed frequency as shown in figure 2.1.

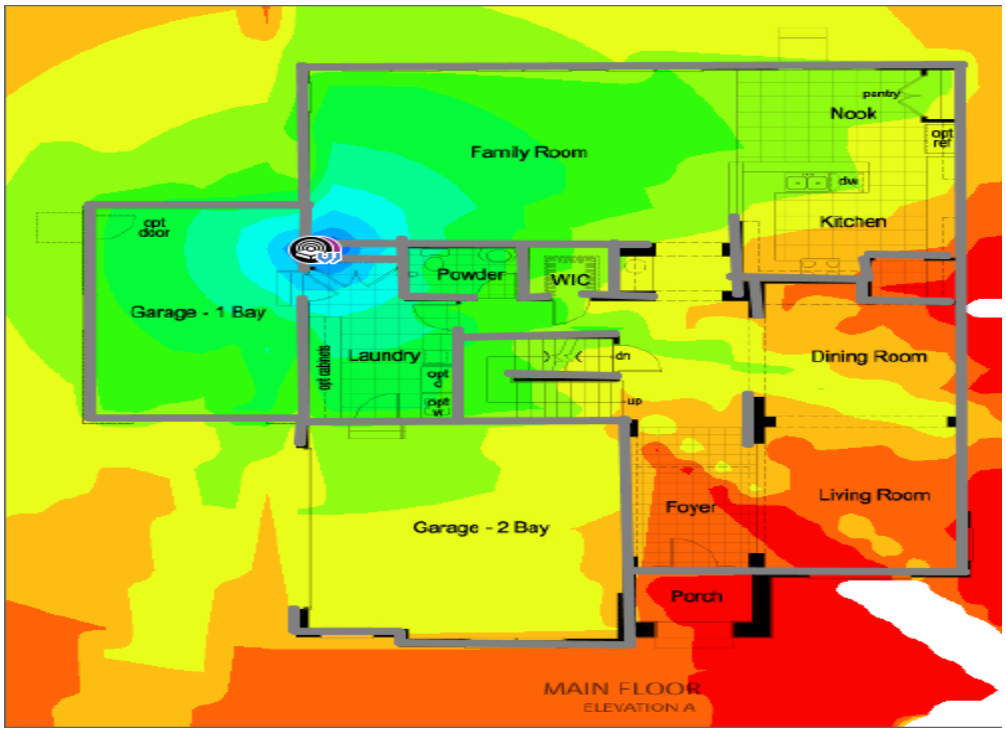

Figure 2.1 Heat map of an indoor wireless environment [31]

The Wi-Fi has a number of standards depending upon the modulation techniques, data throughput, antenna requirements, frequency, and security. The second standard developed in 1997 [7] was 802.11b which uses a frequency of 2.4 GHz and was very weak on security. The later version of IEEE WLAN standard like 802.11n, 802.11b, 802.11g, 802.11ac is much more secure and provides much better coverage with MIMO implementation. 802.11 has a lot of other standards which are improved versions of the previous one depending upon the market requirement, population density, user's preference, cost, data throughput, and market penetration rate. Some of the standards like 802.11a and 802.11n use 5Ghz bandwidth for operations and is extremely effective in multiple tasking.

Wi-Fi has become prominent technologies in the field of broadband internet services competing against the cellular technologies which provides much better coverage. The growing demand in the field of telecommunication and networking have increased the requirement to provide the best suitable service with high-speed data. The cellular technologies provide much better connection, mobility, and coverage in an outdoor scenario, but Wi-Fi is inexpensive in terms of service requirement of the user. It can provide a much higher speed of up to 600 Mbps with 802.11n in comparison 300 Mbps with LTE in the downlink in smaller cell radius with much less cost. The mobile operators are deploying hotspot areas in airports, shopping malls, hotels etc. in order to reduce the cost of large base stations in the cellular world. [7]

Wi-Fi Technology supports a wide range of equipment like smartphones, computers, mp3 players, tablets, printers in dual mode containing different standards together. These

devices are interconnected to the cyber world with the help of wireless adapters for work sufficiently, Wireless routers for clean and quick traffic, wireless bridges for enabling links, PC card, card buses, PCIs and PDAs to improve the range of wireless repeaters. These Wi-Fi devices provide extremely safe networking using a DHCP server, firewall, and interruption detection. [30]

This research paper focuses on propagation modeling of indoor wireless communication scenario. The most common indoor WLAN standard used are 802.11g and 802.11n which supports 2.4GHz for most of the Wi-Fi applications. The research is dedicated to the propagation modeling of Wi-Fi network topology with an indoor arrangement of wireless devices in a relatively smaller radius like office building environment.

2.1.1 Radio spectrum: 2.4 GHz

ISM bands are radio bands that are internationally reserved for industrial, scientific, and medical purposes by Federal Communication Commission (FCC). These radio bands operate in the same frequency increasing the chance of the interference consequently, limiting their operating range to few frequencies. These bands are most suitable for microwave oven, heating applications, near field communication, Bluetooth and Wi-Fi. These bands are unlicensed and are free to use for any user under these frequencies without any rules and regulations [32]. These ISM standards were established in1985 where every device were under the transition from wired cables to wireless standards. This cordless shift of devices led FCC to dedicate certain frequency for their operability in the wireless environment. These frequencies are Type A and Type B based on region

and licensed users. These frequency does not interfere with telecommunication, radio or TV bands and most suited for short-range communication.

The band 2.4 GHz is the most common frequency used in many applications like a microwave oven, short-range communication devices, and Wi-Fi communication due to the wide range of frequency availability from about 2400 to 2483.5 MHz [32].There is a total of 14 channels that are distinct with 5 MHz channel separation for WLAN standard 802.11. The total frequency is separated in Lower frequency, Center frequency and the Upper frequency with each frequency category contains 14 channels each and 12 MHz channel Spacing. The FCC regulations have restricted the use of all 14 channels to just 11 channels. The 2.4 GHz spectrum provides a bandwidth of 20 MHz and which allows the WLAN standards to run different speeds of 1,2,5,11 to 54MBps depending upon the RF modulation scheme. [32]

Radio spectrum 2.4 GHz has much better penetration, range, and cost than any of the Type A and Type B frequencies among ISM bands like its counterpart frequency of 5 GHz for WLAN application. Although 5 GHz provides much higher speed than 2.4 GHz, the indoor environment is surrounded with obstacles which reduce the signal strength of Wi-Fi router. Thus, 2.4 GHz provides much better penetration through obstacles like wall, glasses, man-made interruption and so on. Many WLAN standards are moving towards 5 GHz spectrum as 2.4 GHz is getting crowded with an increase in devices but the 5GHz band doesn’t have the flexibility of a large number of channels as most of the frequency falls out of the ISM bands.

2.2 Propagation Mechanism

2.2.1 General

Propagation mechanisms are important parameters that are analyzed to develop the prediction model. These parameters provide a better understanding of how an electromagnetic radio wave propagates in an environment. The wave behaves in a distinct way depending upon the clutter arrangement like indoor, outdoor, rural, city, sub-urban, hills, lakes, and so on. The propagation parameters are examined on these clutter scenarios to understand the signal coverage, quality, and channel modeling requirements of radio waves. The prediction tools are used to predict the radio propagation based on signal interaction with the real-world objects.

This research paper discusses how an electromagnetic wave interacts with the indoor environment. The radio wave performance changes when it interacts with indoor objects like walls, glasses, man-made objects, tables, chairs and so on. The wave undergoes many changes due to reflection, diffraction, scattering and free space path loss with these objects. These phenomenon are the basis for channel modeling of radio waves in an indoor scenario when signal radiates from a transmitter to receiver. The investigation of these concepts is difficult considering the complete indoor scenario arrangement due to the distinct nature of every indoor setup and distance between the base station and receiver. There are two approaches to investigate these propagation mechanisms: experimental analysis and theoretical analysis. The experimental analysis is done by designing the simplified of an arrangement scenario. The model provides an in general

approach to any indoor setup for measuring these parameters. The experimental analysis requires a large number of hardware and setup for measurements and provides a complex result of many propagation models. On the other hand, a theoretical analysis provides a better understanding of radio behavior with the use of simulation tools. The indoor geometries are specified in a precise manner in a simulation tool and the measurement results are validated for a particular environment. Although it provides a precise measurement data, its validation is limited to a specific geometric condition. This paper focuses on theoretical aspect of propagation mechanism measurement using simulation tools like MATLAB. The theoretical investigation can be achieved using ray tracing theory which interprets radio waves as light waves. The ray theory provides a mathematical approximation to the ray interacting with the environment and depicted as physical entity for scattering, reflection, penetration and diffraction measurement depending upon the frequency and environment condition. [1] The next section describes each propagation mechanisms and illustrates its impact on the radio wave.

2.2.2 Reflection

Reflection of radio waves occurs when a radio wave propagates from one medium to another medium having different electrical properties. The radio waves impose on to the surface medium having dielectric or conductor properties and depending on these material characteristics, the wave is either partially or completely reflected as shown in figure 2.2. If the wave passes through a dielectric, then some of the waves are partially reflected and some are transmitted through the medium. On the other hand, the conductor reflects all the waves to the first medium without any loss of energy. The intensity of the

reflected and transmitted waves are characterized by the Fresnel coefficient which is a function of frequency, polarization, incident angle, and permeability and permittivity properties of a medium [7].The Fresnel reflection coefficient formula is used in a simulation tool for precise prediction of the path loss of a wave [1]. Two ray reflection model is widely used to predict the path loss as it considers both the direct path and ground reflection path between transmitter and receiver. This model accurately predicts the signal strength of the radio wave over a distance of a few kilometers. Some reflection measurements are calculated using the combined equation of transmission coefficient and reflection coefficient which depends upon the incident angle to accurately calculate the propagation of radio wave [1].

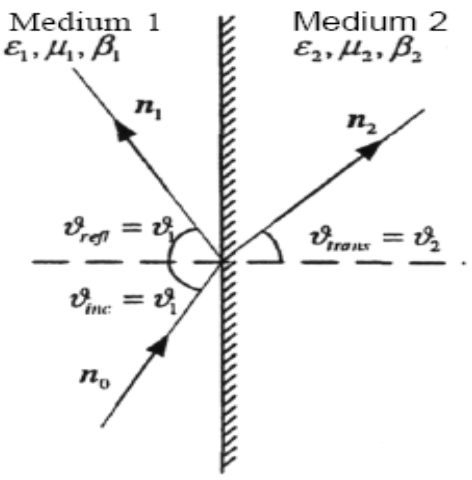

Figure 2.2 Geometry for calculating reflection and transmission coefficient [33]

Snell's Law of reflection suggests that when an incident wave is reflected off a smooth surface, it is equal to the reflected wave and its angle is given as [34]

$$\vartheta_{inc} = \vartheta_{refl} = \vartheta_1 \tag{2.1}$$

When an incident wave is reflected and refracted off a surface, the reflected wave can be defined as [34]

$$E_r = R \cdot E_i, \quad 0 \leq |R| \leq 1 \tag{2.2}$$

Where, $E_r =$ reflected Electric field , E_i = incident electric field and R is the reflection coefficient which is either vertical or horizontal to the incident wave. Snell's law of refraction states that sine of the angle of incidence to the sine of angle of transmission or refraction is a constant which is defined as the refractive index. It is the ratio of speed of light in vacuum to speed of light in medium [34]

$$n_1 \sin \vartheta_{inc} = n_2 \sin \vartheta_{trans} \tag{2.3}$$

Transmission coefficient is represented as follows: [7]

$$E_T = T \cdot E_i, \quad 0 \leq |T| \leq 1 \tag{2.4}$$

Where, $E_r =$ Transmitted Electric field and E_i = incident electric field.

2.2.3 Diffraction

When a radio signal propagates through the curved surfaces of the building, diffraction occurs which decreases the field strength of the signal as shown in figure 1. Diffraction allows a signal to propagate with minimum field beyond the shadowed region. Huygens's principle defines the diffraction process as the vector sum of the electric field of the secondary wavelets in the obstructed region [7]. The principle states that radio waves are moving in the direction of propagation with the help of secondary wavelets generated by the points on the original radio wave front. The secondary wavelets propagate beyond the shadow region once the wave front hits the obstructed region and reach the receiver with

minimum signal strength. This phenomenon is represented in figure 2.3 and 2.4.The scalar diffraction is one of the factors for wavelength dependency of antenna aperture in Friis Equation. In radio communication, the signal undergoes many diffraction loss before reaching the receiver as the number of signal wavelets transmitted gets blocked by the curved edges reducing the Fresnel zone of the radiated signal. All the diffracted signals are combined in the vector form once it reaches the receiver to produce a signal with minimum signal properties. The vector sum of the signal depends upon the geometry of the environment as it depicts the number of diffraction occurred from the transmitter and receiver.

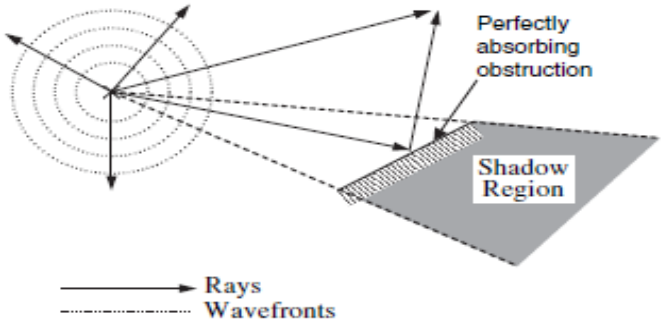

Figure 2.3 Illustration of diffraction [33]

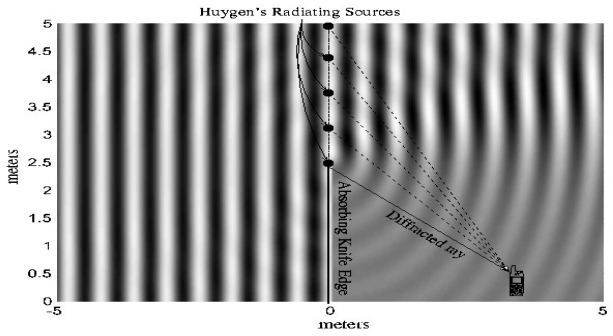

Figure 2.4 Demonstration of Huygens's Principle [33]

Knife-Edge diffraction as shown in figure 2.5 and multiple knife-edge diffraction models are commonly utilized by the simulation tools to predict the path loss of the signal. These models treat the obstructed objects as the diffraction knife edge and are based upon on the theoretical approximation of the diffraction losses. Although precise prediction of diffraction loss is very difficult, these models provide a close approximation of loss by providing the order of magnitude of its loss. Fresnel equation provides the electric field strength of diffracted wave with respect to free space field strength as : [7]

$$F(v) = \frac{(1+j)}{2}\int_{v}^{\infty} \exp\left(-\frac{j\pi t^2}{2}\right) dt \tag{2.5}$$

where v is the diffraction parameter.

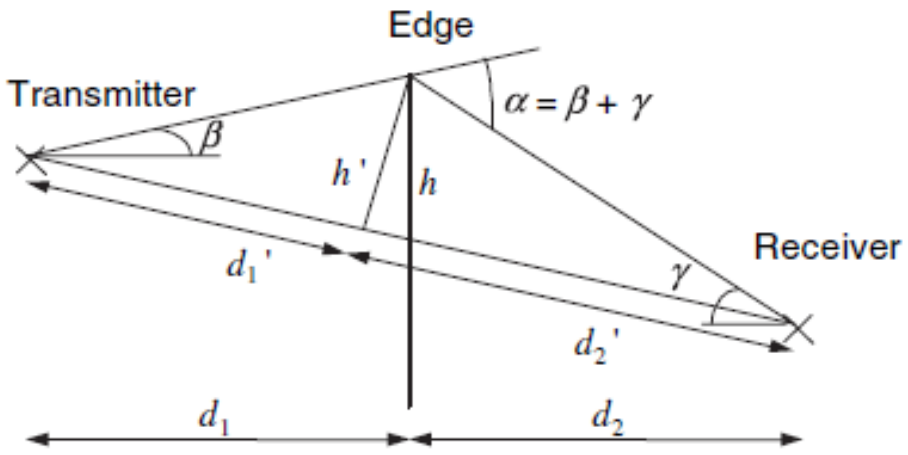

Figure 2.5 Knife-Edge diffraction geometry [33]

Diffraction Parameter is given by [7]

$$v = h\sqrt{\frac{2(d_1 + d_2)}{\lambda d_1 d_2}} \tag{2.6}$$

Where d_1 is the distance between obstruction and transmitter, d_2 is the distance between obstruction and receiver and h is the height of obstruction. The multiple knife-edge model provides a vector sum of all the diffraction caused by the multiple knife edges in comparison to the single knife edge diffraction loss. [7]

2.2.4 Scattering

The radio waves scatter when a wave is an incident on rough surfaces and surfaces which has much less wavelength than the incident wave as shown in figure 2.6. These surfaces spread out the signal in all the direction when it leaves the incident surface. The signal is dispersed in all the direction which reflects some of the signals in a specular direction. The signal received after diffraction and reflection do not provide the actual signal strength. The diffused signal after scattering always add up the spread-out signal to provide an additional signal strength [7]. Conversely, the definition of scattering describes there is a reduction of signal in specular direction after reflection. The concept of scattering has been studied for an indoor environment to investigate the indiscretions of scattering with building walls [35].

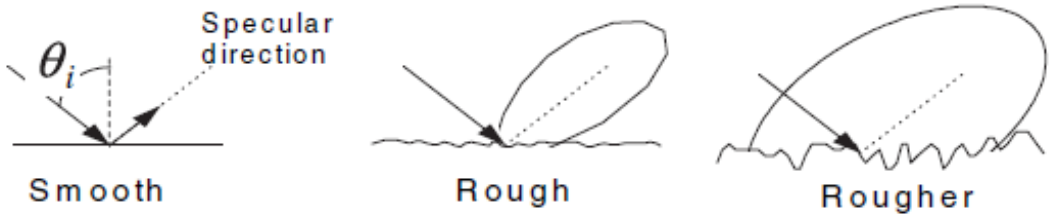

Figure 2.6 Illustration of scattering in various surfaces [33]

The roughness of the surface is examined using Rayleigh criteria. The critical height h_c, of surface protuberances at an angle of incidence .This height depicts the protuberance of the surface and is represented by the equation [7]

$$h_c = \frac{\lambda}{8\ sin\theta_i} \tag{2.7}$$

2.2.5 Transmission and absorption

When a signal propagates through a material, it gets refracted in the sense that some of the signals get reflected and some get transmitted over the material in the direction of the receiver. The reflection of a signal has been reviewed in the above section. The main discussion lies in the transmission of a radio wave through building materials and its absorption while propagation towards the detector. The transmission of radio waves is characterized by the transmission coefficient, electrical properties of building materials and angle of incidence of the signal to the material. The absorption of waves is caused by ohmic heating, the angle of incidence of wave and attenuation rate [36].The ohmic heating phenomenon heats the flux lines of the ray coming from the source and attenuated its propagation. The absorption loss measurement is difficult as the materials are non- homogenous. The non-homogeneous nature of materials like the mixture of materials like in wood and bricks, the density of the materials and porosity of the material amplifies the absorption loss [36]. The homogeneities of a material are characterized by comparing its wavelength with the material and including a dielectric constant to define a material if it is small. The materials like glass are considered homogenous in nature and

do not require a dielectric constant whereas the multi-layered materials like double glazed windows, cavity walls and many are irregular in nature. The concept of transmission coefficient is used in double glazed glass and found attenuation of the signal of greater than 3dB from approximately 1 GHz due to its dependence on the frequency [36].Also, the amplitude and phase of the signal fluctuations dependent to the angle of incidence of the wave. These losses are difficult to include in the propagation models and thus precise measurement is not achieved. The fluctuation in transmission coefficient is due to the refractive nature of the materials and its dependence on the phase of the signal while no such fluctuation occurs for absorption loss [36]. The absorption loss is also caused by frequency, but its dependence is almost negligible compared to the loss caused by the dielectric of the materials. It is necessary to analyze every modern building materials and include their behavior in the prediction models to accurately understand their propagation. This thesis research considers the homogeneous materials used in indoor building materials like wood, glass, and concrete. The dielectric nature is constant over the entire surface of the materials measured and its behavior with the different frequencies are taken into account. The table depicts the typical loss of the material under 2.4 GHz and 5 GHz conditions [37]:

Table 2.1 Typical indoor material loss at 2.4 GHz

Material	Loss (dB)
Wood	3-4
Glass	2-3
Brick/concrete	6-18
Double pane coated glass	13
Cubicle wall	5

Table 2.2 Typical indoor material losses at 5 GHz

Material	Loss (dB)
Wood	6-7
Glass	6-8
Brick/concrete	10-30
Double pane coated glass	20
Cubicle wall	4-9

The signal attenuation for every material construction has increased effect for 5 GHz in comparison to the 2.4 GHz due to the wavelength dependence of transmission and reflectance coefficient.

2.2.6 Friis equation: free space path loss model

In radio communication, the Friis Transmission equation is used to calculate the power received by one antenna under idealized condition (unit gain) when transmitted from another antenna separated by a certain distance while operating at a certain frequency [38]. In free space medium, the equation can be written as follows:

$$P_R = \frac{P_T\, G_T\, G_R \lambda^2}{(4\pi\, R)^2} = \frac{P_T\, \lambda^2}{(4\pi\, R)^2} \tag{2.8}$$

Where P_R: power available at the input of the receiving antenna, P_T: power to the transmitting antenna, R: distance between the antennas, G_T: the antenna gains (with respect to an isotropic radiator) of the transmitting antennas, G_R: the antenna gains (with respect to an isotropic radiator) of the receiving antennas and λ : Wavelength. [38]
In this thesis, gain of transmitter and receiver in the equation 2.7 is considered as one which is the ideal condition.

2.3 Indoor Propagation Model

2.3.1 General

It is important to characterize the channel of the propagating wave in an indoor wireless communication system to achieve the maximum signal strength and quality of radio wave. The radio waves propagate in a different way in comparison to outdoor propagation environment. Indoor systems consist of a large number of obstacles like walls, furniture, building materials, human movement and so on. Also, the distance between the different obstacles is extremely less which causes more signal attenuation due to the shorter delay spread. These hindrances change the characteristics of a radio wave as it tends to diffract, reflect and scatter when it interacts with indoor materials. The diffracted, scattered and reflected wave reaches the receiver location in more than one path causing a multipath. The multipath causes deep fading and spreading of the signal pulse which consequently, produces interference in the propagating wave [35]. Outdoor propagation scenario differs from an indoor system because it has a much larger distance coverage area, large obstructions like hills, trees, tall buildings etc., fast human movement and so on. Thus, it is necessary to design a propagation model which is detailed for an indoor environment. The outdoor propagation model is designed for an outdoor scenario which is more empirical in nature while indoor propagation demands a site-specific propagation model to precisely predict the path loss parameters like wide-band, time-variation, and empirical characteristics [1]. Indoor propagation model can be characterized into two main categories: Empirical model and deterministic model. Empirical models are designed based on theoretical assumptions using a mathematical

equation. This approach provides an in-general propagation technique to identify the signal attenuation measurement. The model considers wave characteristics like delay spread, time variance, wall losses, frequency dependence, the distance between transmitter and receiver, variable factor to define the propagation mechanisms, power delay and many more [1].These factors are defined within certain threshold value to provide the best prediction result in any indoor-scenario. Although all the factors are considered in an empirical model, the precise estimation of path loss is difficult in an indoor system due to different structure and materials used in different estimation. This problem can be limited with the use of a site-specific deterministic models. A deterministic model considers the detailed structure of an indoor environment which physically simulate the wide-band and narrow-band information of a channel to estimate the path loss. Deterministic approach ignores the extensive measurement method of empirical model and provides a much exhaustive information of signal propagation in a specific surrounding. A typical measurement of channels requires a much wider range of equipment, power, human resources, which subsequently increases the capital of the planning process. A deterministic model provides a much economical simulation method for planning engineers. This research focuses on designing a Semi-deterministic propagation model involving features from both empirical and deterministic methods.

2.4 Empirical Models

Extensive research has been done on designing a propagation model to characterize the indoor radio propagation. There are a lot of empirical models which are commonly used in for radio coverage planning like the empirical narrow-band model, empirical wide-

band model, cost-231 Hata model for an indoor scenario, wall count model and so on. [1, 5, 6, 9-11] All these methods use the experimental data to predict the path loss. The simplest empirical propagation model can be defined as the free space path loss model which depends on the frequency, aperture area and distance of between transmitter and receiver. It only gives the path loss prediction of radio waves in free space environment excluding all other obstruction in an indoor system. The received power relation in fig 2.7 depicts the loss with distance from Friis equation.

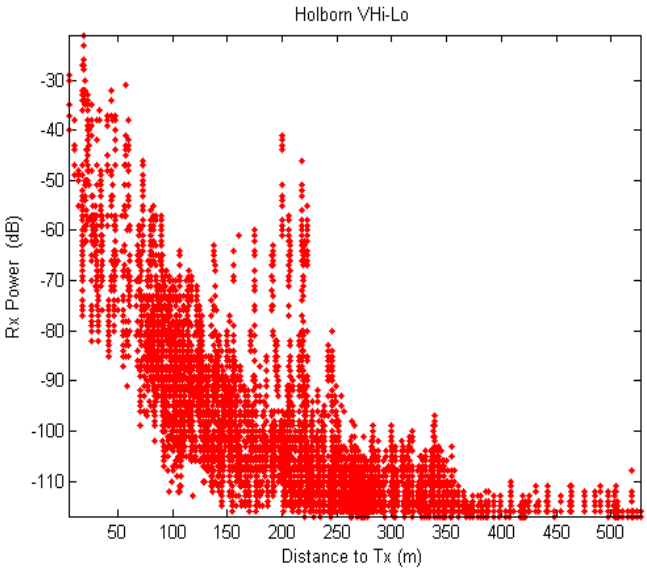

Figure 2.7 Inverse relation of received power with distance [33]

The empirical narrow-band consists of simple models like the COST 231 one-slope model, COST 231 multi-wall model, and COST 231 linear attenuation model. One slope model is extremely easy to use as it only depends on the path loss and logarithmic distance. One slope model can be expressed as [1]

$$L = L_0 + 10\, n \log(d) \tag{2.9}$$

where L_0 is the path loss at 1-meter distance, n is the power decay index and d is the distance between transmitter and receiver .The second model is Linear attenuation model which indicates linear relation between loss and distance. The value α indicates the attenuation coefficient in dB/m and d is the distance between transmitter and receiver. The model is represented as :

$$PL = L_{FSL} + \alpha d \tag{2.10}$$

The previous two models doesn't consider loss related to penetrated walls and floors. They are only a dependent factor of distance between transmitter and receiver.

The third model is the mutli-wall model which includes input parameters of walls and floors losses along with the free space path loss. The wall and floor loss are characterized by an empirical factor. Multi-Wall Model can be expressed as [1]

$$L = L_{FS} + L_c + \sum_{i=1}^{l} K_{wi} L_{wi} + K_f^{[(k_f+2)/(k_f+1)]-b} \; L_f \tag{2.11}$$

where,L_{FS} is the free space loss, L_c is the constant loss , K_{wi} is the number of penetrated walls,L_{wi} is the loss of wall type i , K_f is the number of penetrated floor , L_f is the loss between adjacent floors , b is the empirical factor and l is the number of wall type.

The loss factor includes loss like furniture and corridors. This approach takes into consideration every wall and their corresponding loss between transmitter and receiver which consequently, includes all the non-linear loss estimation of an individual wall. Conversely, the penetration loss of floors is considered linear and thus, does not provide a precise approximation. Another empirical model is WINNER II model. The model was considered for indoor to outdoor, outdoor to indoor and mostly for outdoor scenarios. The

model is suitable for 2 GHz and 5 GHz and is developed for both LOS and NLOS conditions. The LOS formula can be represented as : [39]

$$PL = 18.7 \log(d) + 46.8 + 20 \log(f_c/5) \tag{2.12}$$

where,d is the distance between TX and RX in meters and f_c is the frequency in GHz. NLOS formula can be depicted as : [37]

$$PL = 20 \log(d) + 46.4 + 20 \log\left(\frac{f_c}{5}\right) + 12\, n_w + F_L \tag{2.13}$$

where, d is the distance between TX and RX in meters and f_c is the frequency in GHz and floor loss is represented as

$$F_L = 17 + 4(n_f - 1) \tag{2.14}$$

Where, $n_f$is the number of penetrated floors. The NLOS equation shows linear and constant relation of loss with floors and walls. The wall loss increased by 4 dB and floor loss by 12 dB. [40] ITU-R M Model is another empirical model which estimates the path loss of a propagating wave.[41-46]

$$PL = 16.9 \log(d) + 32.8 + 20 \log(f_c) \tag{2.15}$$

where, d is the distance between TX and RX in meters and f_c is the frequency in GHz. Some other empirical band models are used to predict the impulse delay spread, and power delay spread [10, 11]. Cost-231 Hata model is extensively used for outdoor propagation modeling of channels but with the increase in demand for indoor channel modeling, it has been designed to predict the signal characteristics in an indoor radio system. It is widely known as PCS Extension of Hata Model [7]. It takes into account parameters like distance, frequency, the height of the receiver and transmitter, and a constant which depends on the cluster size of the environment. Some researchers have designed new empirical models combining some of the features of each model to design a

more optimized version for precise measurement. Four empirical models has been compared in different scenarios to find the best model to predict the path loss. Two models considered takes into account the losses due to walls and two models shows linear relation with distance. In the first scenario, the UE and access point are in LOS condition and the maximum distance considered is 6m. The frequency used to predict the path loss is 2.4 GHz. The path loss exponent for Cost-231 MWMF model is 4. The LOS equation for ITU-R model has been considered and the attenuation coefficient is considered to be 0.4 for linear attenuation model. The figure 2.8 represents path loss estimation of all the models shows close approximation with each other. The cost 231 linear attenuation model estimates path loss close to 60 dB while other models lies close to 55 dB.

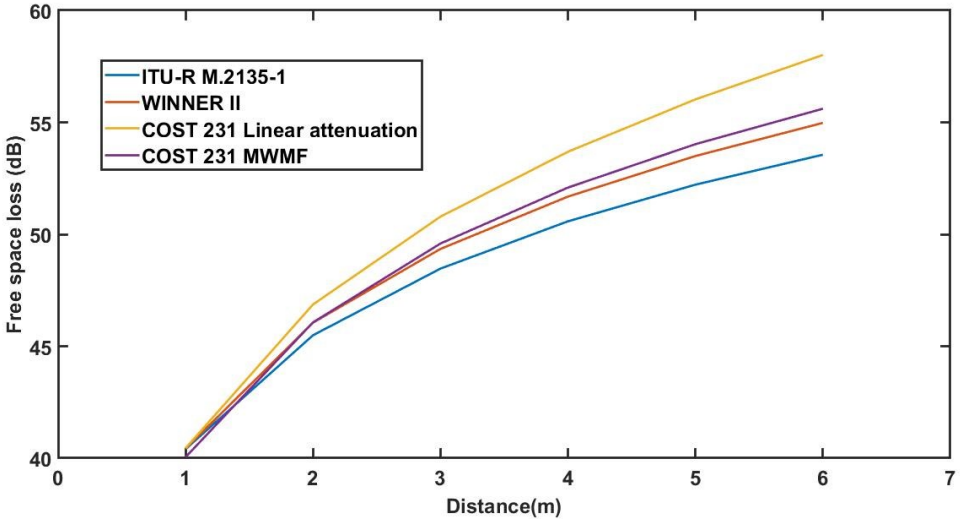

Figure 2.8 LOS condition at 6.5 m

In the second scenario, the UE and access point are in NLOS condition with two walls between transmitter and receiver at 2m and 5m location as shown in fig 2.9. All the parameters are same except NLOS equation has been considered for ITU-R model. The

wall loss for Cost 231 was considered to be 8 dB and 5 dB. The graph shows that for WINNER-II model and Cost 231 MWMF model considers the effect of walls and other two models shows the same path loss from scenario-1. Comparing two models which takes into account the effects of walls , WINNER-II model shows linear and constant effect of walls that is 12 dB while Cost 231 model has non-linear effect of walls as it accounts the loss for individual walls.

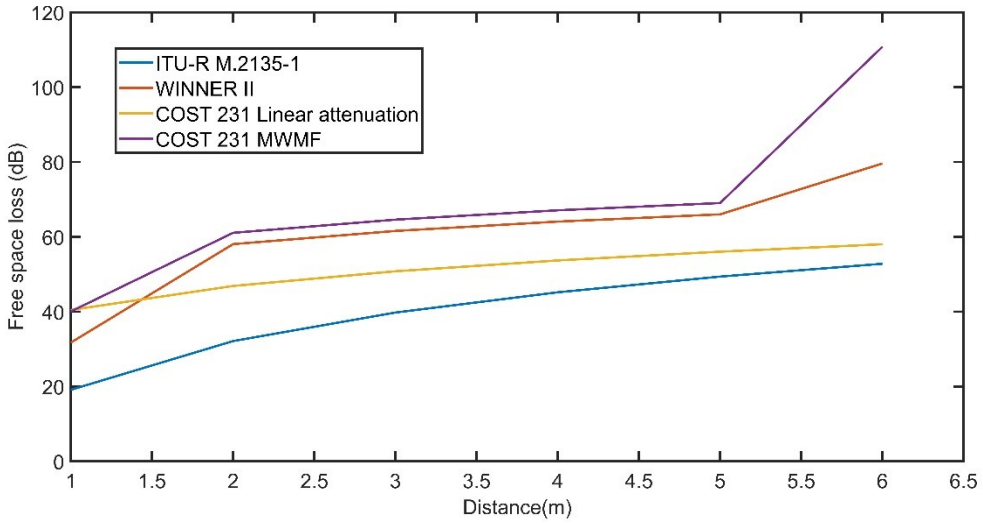

Figure 2.9 NLOS condition with two walls

In the third scenario, distance between transmitter and receiver is 10 meters and there are three walls. The wall losses for COST 231 model is considered to be 8 dB,5 dB and 6 dB. All other parameters considered are same as scenario-2. The path loss has increased for all the models due to the increase in distance but WINNER-II and COST 231 MWMF model shows abrupt increase in loss due to the walls. Similarly to scenario-2, the Cost 231 model provides a much better effect of each walls for the estimation of loss. ITU-R

and Cost linear attenuation model shows path loss estimation with distance and constants while not taking into account any effects of walls while WINNER-II model showed constant loss with every wall. Consequently, COST 231 MWMF shows non-linear signal attenuation with different building material losses. Accordingly, this thesis considers the empirical cost 231 MWMF model in equation 2.10 for path loss estimation while ignoring the effects of floors.

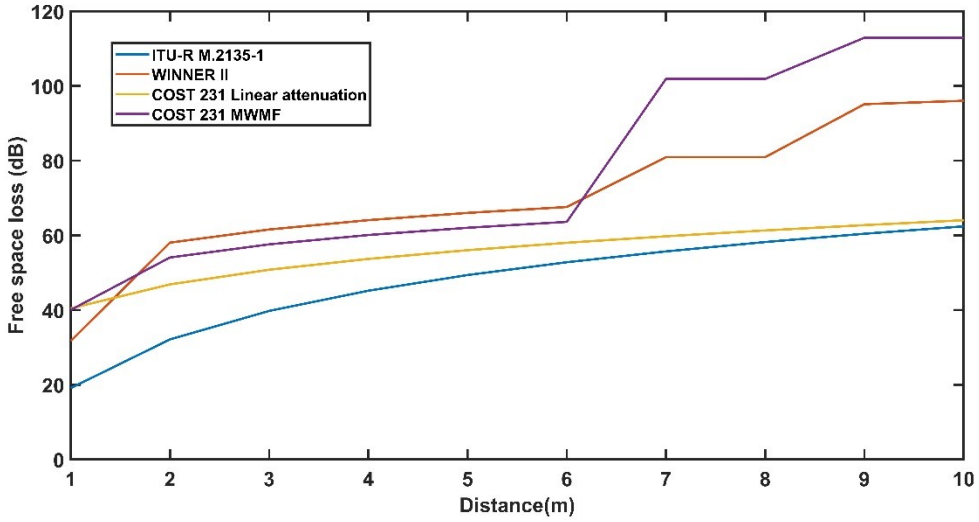

Figure 2.10 Three Walls between UE and TX

The model is based upon free space path loss and loss of walls between transmitter and receiver. The constant loss and penetration loss due to the floor is not taken into account. Thus, the considered equation for path loss can be represented as

$$L = L_{FS} + \sum_{i=1}^{l} K_{wi} L_{wi} \tag{2.16}$$

In this thesis, a simple propagation model is considered to investigate the behavior of radio wave propagation under the perception of a human eye. The model will help to

estimate the path loss of radio wave by correlating light wave as observed by human eye. The complexity of thesis research lies in correlating radio wave with photometry which is discussed in chapter-4 which focusses on the concept of measurement of light with the weighted response of human eye.

2.5 Deterministic Models

When a system requires a physical simulation of indoor radio waves, deterministic models are the best option where several parameters like path loss, the angle of arrival and impulse response [1] can be computed at the same time. These models are more advantageous than the empirical model and typical experimental measurement as it predicts precise radio propagation and remove complex planning requirements respectively. Deterministic models are site-specific which requires detailed information about building structure like GIS vector indoor map that includes all the data of a particular environment. These information helps to simulate the radio wave propagation with all the prediction parameters. There are many deterministic models available in the 21st century which are based upon two main methods: finite Difference domain technique and geometrical optics technique [1]. This research is mainly focused on geometrical optics method which is based on the concept of an electromagnetic wave behaving like a ray. The power source defines the number of rays coming from a radio wave and the receiver validates the signal strength of the wave with the number of ray lines reaching the destination. The number of rays at receiver helps to estimate the indoor radio coverage once it interacts with the environment undergoing diffraction, reflection, scattering and transmission loss. The transmission and reflection of signal waves are

characterized by the permittivity of the material used which is defined by transmission and reflection coefficient respectively. These coefficients describe the level of signal attenuation caused by propagation mechanisms. The signal attenuation is also affected by other factors like the angle of incidence and relative polarization [35]. Ray-launching or ray-tracing technique and image techniques are the two most common approach to geometrical optics [14].The two methods are the basis for any physical simulation and are discussed briefly below.

2.5.1 Ray launching method

The ray-launching technique includes all the information about the indoor environment like transmitter location, receiver location, walls, furniture, ceilings, floors, and partitions. The transmitter and receiver location is allocated a three-dimensional coordinate while other data are depicted by plane surfaces of relative thickness and material permittivity [35] as shown in fig 2.11. The concept involves launching of rays from the transmitter location and counting the rays acknowledged at the receiver. The rays from the transmitter either gets reflected or transmitted of the plane surfaces depending upon the intensity of wave from the source. The transmitted ray is located at every intersection point caused by any plane surfaces until the amplitude of the ray reaches a specific threshold. The threshold is defined by the user as the minimum number of intersection applicable according to theoretical assumptions relating to different parameters that define a plane surface. The ray can be analyzed for scattering and diffraction in a similar manner to the angular reflection at the same time. [1]

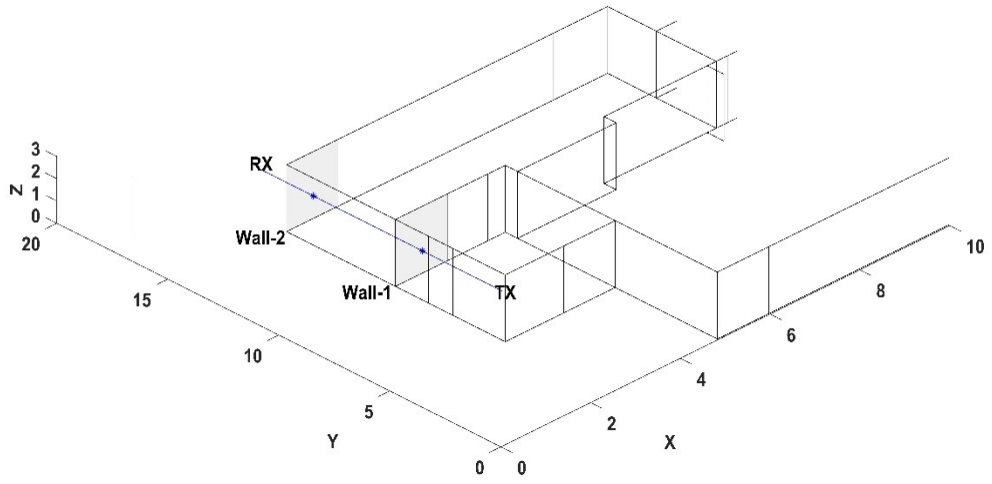

Figure 2.11 Ray tracing in an indoor building

2.5.2 Image approach method

In an image approach method, all the data are referenced by the three-dimensional coordinates including plane surfaces. The image provides the coordinates for all the data information and rays from the transmitter are relatively traced for every image locations like walls, corridors, floors, and ceilings. A single ray is transmitted from the source and the specular reflection is analyzed with its interaction with the plane surface. The point of interaction of ray with the surface is the point of reflection. The first order of reflection occurs when a radio source ray intersects the first planar surface. Similarly, the second order of reflection takes place when the first order reflected ray passes through another plane surface. Thus, the order of reflection is defined by the number of plane surfaces between the source and receiver location. The reflected way starting from the source to receiver is called forward ray-tracing and vice-versa is called backward ray-tracing [35].

As the order of reflection grows, the calculation time increases due to complex tracing process. [1]

This research is based on a semi-deterministic model which considers the image approach technique. The direct path and its interaction with the plane surfaces are calculated with deterministic approach while the complex computation like free space path loss and loss of walls are computed using the empirical model. The combined approach of empirical and deterministic model enables to utilize the best features of both techniques. It removes the complexity and cost of the measurement requirements and provides much precise result compared to individual models for indoor radio propagation. The concept of this propagation model is to find the number of the interaction of rays with the indoor environment which defines the number of walls between transmitter and receiver and their losses are added with the free space path loss to determine the actual path loss.

2.6 GIS Vector Data

Radio frequency propagation modeling is an important tool for estimation of location, coverage, power, and quality. The algorithm is based on an empirical or deterministic approach which helps to design a prediction model based on empirical data and assumptions of path loss. A proper implementation of these models is provided by a geospatial information system (GIS). GIS data contains all the geographic and architectural information such as building materials, their size, location, floor plans, the orientation of the building and plenty of others as shown in figure 2.12 [47]. These information can be used to estimate the proper positioning of the building materials and

obstruction without error. This thesis research utilizes data file generated from the GIS tool system that includes features like coordinates, digital information, points, polygons, and multi-patch of the indoor building environment [47]. The multi-patch feature generates a three-dimensional model by adding the characteristics of height in a two-dimensional building data. The multi-patch data uses the concept of class data which assigns a table to each building materials for data storage. The Table contains information like building material ID, location, size, and material type to define its impact in the data file. In this thesis, GIS data is used to predict the path loss of the indoor building using MATLAB with a semi-deterministic algorithm. The geometrical concept of plane-line intersection is considered to predict the intersection of source ray line with materials and obstacles defined in the multi-patch GIS data.

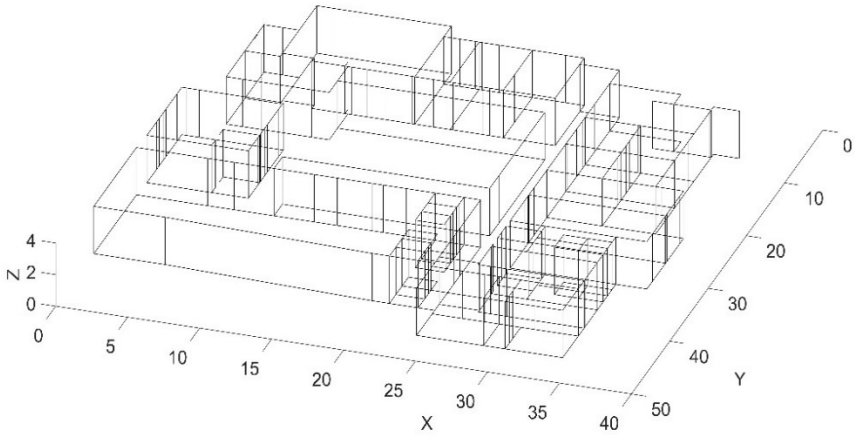

Figure 2.12 GIS Vector map of an indoor building

3. INTRODUCTION TO LIGHT WAVES

3.1 General Overview

Electromagnetic (EM) wave radiates from a source in a space environment. Their propagation is characterized by the interaction of wave with several objects and obstruction. The waves in EM spectrum have different wavelength but their propagation is obliged to face mechanisms like reflection, transmission, diffraction, and scattering as discussed in propagation mechanism section. These mechanisms change the structure of wave on the process and consequently, the receiver cannot utilize the proper intensity of the wave coming from the transmitter. The proper measurement of the EM wave is necessary to analyze the signal intensity level and factors affecting the signal propagation. The phenomenon of measuring and detecting wave in visible light distribution, low-frequency radio waves, infrared, and ultraviolet of the EM spectrum is called Radiometry. It predicts the power distribution of light wave in space. The concept of measuring and detecting the level of light intensity with respect to the human eye is called Photometry. Photometry is a subclass of radiometry which is related to the perception of a human eye in the visible spectrum. The spectral distribution of light in the EM spectrum is significant as the wavelength is a dependent factor when the light propagates through different materials like dielectric, conductors etc. The optical properties of the materials and wavelength decide the propagation mechanism characteristic like reflectance, transmission, and absorption [48]. The spectral distribution of visible light does not have a precise limit as it varies from one person to another. The human eye can perceive the light of wavelength from 360nm to 830nm and radiation of

single wavelength from this range in optical measurement is called monochromatic light source. The human eye is most sensitive to 555nm in wavelength and it is considered the most suitable monochromatic light source for 100% perception of the light illuminated or reflected from the source.

It is important to understand the concept of solid angle when dealing with radiometry and photometry measurements. The solid angle is the angle at which the light gets illuminated from the source or reflected of the surface in a particular angle depending on the type of source. If two plane lines get intersected at some point, a plane angle is subtended between the two lines. Similarly, if the plane line lies inside the circle, the solid angle is the radial projection of the two planes lines with respect to the radius of the circle [48]. Solid angle is the ratio of the area of a segment from a unit sphere to the square of the radius [48] and is represented as follows:

$$\Omega = \frac{A}{R^2} \tag{3.1}$$

where A=area of subtended surface and R= radius from a point source to apex area Thus, it can be determined that a sphere with unit radius subtends a solid angle of 4pi steradian from above equation. It is a geometrical quantity that predicts the amount of light projected or reflected in a particular field of view from a point source. The subtended angle defines the area covered by the light source on a particular surface. The amount of light coming from a point source subtending from a curve or apex angle is the measure of the size of the image. Although, the solid angle is dimensionless, and it has been assigned a unit called Steradians (sr) for measurement assistance.

3.2 Radiometry

Radiometry is the concept of measuring light in EM spectrum which includes two aspects of its measurement: theoretical and practical method. The practical process includes measurement of light using instruments and materials like photodiodes, photodetectors, thermocouples, vacuum phototubes, photosensitive materials and plenty of others. [49] The theoretical methods include the concept of radiant energy, radiant flux, radiant flux density, radiance intensity, radiance, and irradiance to define light. This thesis research is interested in the theoretical aspect of measurement to understand the propagation characteristics of a light wave. The radiometry measurement is constructed on two quantities that define the source of the light wave, radiant energy, and radiant flux. Similarly, its interaction with objects in the environment is characterized by radiance, irradiance and radiant intensity with respect to the surface area of the source and receiver. It is necessary to understand these concepts to have the deep sense of light wave propagation and is discussed individually below.

3.2.1 Radiant energy and spectral energy

Electromagnetic wave transfers energy while propagating in space. This energy is quantified as the radiant energy which is either coming from the source, going onto and through the surface. This energy contains all the wavelength of the light source. Spectral radiant energy is the radiant energy with respect to a wavelength interval at a specific wavelength. Whether the light source is monochromatic or multiple wavelengths, it is stated in Joule [48].When a light signal radiates through space and gets attracted by the objects, its energy characteristic changes. The radiant energy is converted into some other

forms like thermal or kinetic energy [49]. Thus, radiant energy explains the rate of flow of energy, flux density and total energy emitted in a specified period of time to understand the features of the light signal. The radiant energy is depicted by the symbol, Q.

3.2.2 Radiant flux and spectral radiant flux

Radiant flux is defined as the power and is described as the quantity of radiant energy flowing on a surface per unit time [48]. The flux is measured in Joule per unit time or watts. The radiant energy is the geometrical ray lines coming from the light source and the amount of these light rays falling on a surface per unit time is flux. The amount of ray lines on the surface is always proportional to the total amount of current measured over a period of time [49]. The radiometry equipment like photodetectors detects the amount of light falling on its surface to measure the radiant power. The spectral radiant flux is the amount of radiant flux per unit wavelength interval at a specific wavelength and is measured in Watt per nanometers. Radiant flux is denoted as,Φ.

$$\Phi = \frac{dQ}{dt} \tag{3.2}$$

where dQ is the radiant energy.

3.2.3 Radiant flux density: Irradiance

Radiant flux density is the radiant flux per unit area at a point in a specific surface [50]. It is dependent on the position of flux on a specified surface. Radiant flux density,

Irradiance is measured in watt per square meter. The irradiance incident on a specified surface gets reflected in all the directions and is called *exitance*. Irradiance and exitance can be measured at any position and have the same units. The difference lies in the direction of rays, either coming from the source or leaving from the surface. The spectral radiant flux density is radiant power per unit area per unit wavelength interval at a wavelength, lambda at a point on a specified surface [48]. It is denoted by, E.

$$\mathrm{E} = \frac{d\Phi}{dA} \tag{3.3}$$

where $d\Phi$ is the radiant flux and dA is the area of the surface.

3.2.4 Radiant intensity

Radiant Intensity is defined as radiant flux per unit solid angle. The radiant flux is the amount of ray lines coming from a solid angle incident on the surface, transmitting through or reflected of the surface[48]. The receiver or detector receives the light rays subtended by the solid angle of a plane, circle or sphere surface. The angle subtended by a hemisphere is 2pi and a sphere is 4pi. For example, the radiant flux in a sphere environment has ray lines of 4pi steradians neglecting the isotropic rays in all the direction from the source. Radiant intensity is applicable to point sources like lamps while it is not appropriate for extended sources like sunlight. The radiant intensity depends on factors like a point source, the direction of the point source and the direction of the surface at which it is incident [48] It is measured in watt per steradian. Radiant Intensity is denoted by I, and defined as:

$$\mathrm{I} = \frac{d\Phi}{d\omega} \tag{3.4}$$

where $d\Phi$ is the radiant flux and $d\omega$ is the solid angle emerging from the point source.

3.2.5 Radiance

Radiance is the radiant intensity per unit incident area. It is the radiant flux incident on a surface area projected from a solid angle of a point source on a specific surface. The radiant flux depends on the factor like a point source, the direction of a point source, the direction of specified surface and position of the specified surface with area. It is the amount of radiant flux lines coming from a point source in a cone-like structure having a solid angle, omega. Radiance is measured in watts per square meter per steradian and is represented by, L. Radiance is defined as [48]

$$\mathrm{L} = \frac{d^2\Phi}{d\omega\ dA} \tag{3.5}$$

3.3 Photometry

Photometry is the branch of radiometry that is used to measure light in the visible portion of EM spectrum with the weighted human eye response. The human eye response is characterized by the eye sensitivity function that defines the perception of light in the visible spectrum. The empirical approach of human eye response is the basis for perceiving light in photometry measurements contrasting itself from radiometry [49]. As discussed in the previous section, the human eye system can operate in the wavelength ranging from 360nm to 800nm, unlike radiometry which deals at all wavelengths. The

eye response varies from one person to another due to its nonlinear [49] reception of wavelengths especially ranging from 360nm to 410nm towards lower limits and 720 nm to 800nm in upper limits. The green-yellow light at 555nm is considered the most sensitive wavelength for human eye response. A source of this wavelength will appear much brighter to the human eye than other wavelengths in the visible spectrum. The limit of visible spectrum varies according to the sensitivity of a person as some people cannot see light in lower and upper limits. The human eye is a complicated system as its sensitivity depends on wavelength, amount of radiant flux, the source is whether point or extended and whether it is constant or flickering, the environment condition and other factors [49]. All these factors must be considered for the precise measurement of human eye perception. The human eye response to different wavelength is characterized by receptors in the retina of an eye. These receptors are responsible for converting the radiation energy coming from the source into chemical signals for the neural system. The retina has two receptors called cones and rods. These receptors are active depending upon the brightness of the surrounding. The cones are suitable during daylight condition with sufficient amount of brightness in the environment and are called photopic vision. While rod cells are active during the night where the amount of radiant flux in the environment is very low. This type of vision is called scotopic vision. Thus, these receptors are an influencing factor for the sensitivity of an eye with respect to wavelength along with the spectral transmittance of the retina [48]. The eye changes its vision from rod to cone and vice-versa depending upon a certain threshold range which is called mesopic vision. The Mesopic vision is the combination of photopic and scotopic vision towards low-light condition and provides a transition for receptors. This research is focused on the photopic

vision of the human eye under normal lighting condition. The International Lighting Commission in 1924 [48] standardized a weighted response function for the human eye with respect to different wavelength. This function is called the CIE spectral luminous efficiency function [48]. This function is represented by V(lambda). The spectral response curve for the photopic vision is given by this graph:

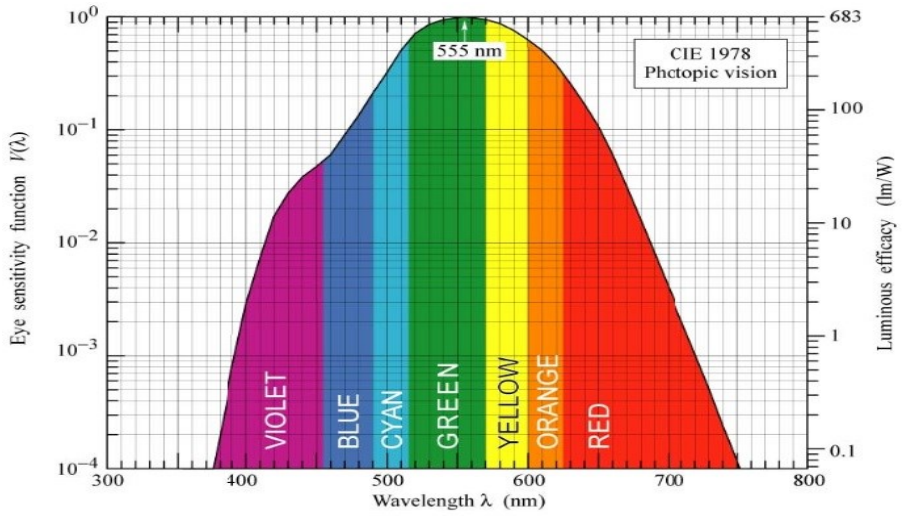

Figure 3.1 Photometric Spectral Luminous efficiency function curve of CIE standard.[51]

The graph illustrates that the eye sensitivity function is unity at 555nm and tends to decrease on either side of the wavelength limits. Similarly, spectral response curve for photopic and scotopic vision is also standardized by CIE commission for human eye sensitivity under low light condition. The luminous efficacy defined as the ratio of luminous power to the radiometric power and is measured in lumen per watt.

3.3.1 Photometric Quantities

Photometric concepts are equivalent to radiometry apart from the sensitivity response of human eye. Luminous energy is the photometric radiant energy and provides the basis to understand the concept of luminous quantities. The Luminous energy can be defined as [48]

$$Q_v = 683 \int_{380}^{770} Q_\lambda \, V(\lambda) \, d\lambda \tag{3.6}$$

Where $V(\lambda)$ is spectral sensitivity of eye, Q_λ is the spectral radiant energy and 683 lumen/watt is the scaling factor from the definition of candela. Conferring to the definition of candela given by [48] General Conference on Weights and Measures, a light propagating at 555nm has 683 lumens per watt. A point source has a luminous intensity of one candela according to international conventions. The conversion of the radiometric energy to luminous energy provides a foundation to change other quantities to luminous form. Thus, the luminous radiant flux can be written as follows :[48]

$$\Phi_v = 683 \int_{380}^{770} P_e \, V(\lambda) \, d\lambda \tag{3.7}$$

Where Φ_v = luminous flux and P_e= radiant flux in watts.

3.3.2 Luminous flux

Luminous flux is the photometric counterpart of radiant flux [48]. The radiometry states the radiant flux as the source of power in watts while in photometry the flux is defined by lumens. A lumen is the luminous flux of unit candela produced by a light source over a

solid angle in steradians [48]. The luminous flux is dependent on the light source and the spread of energy over time. Spectral response of the luminous flux is the weighted power of the source over the interval of wavelength. Luminous power at a point source is defined as [50] :

$$\Phi_v = 4\pi I = I\Omega \tag{3.8}$$

Where I is the luminous intensity in candela and 4π is the steradian angle of a sphere.

3.3.3 Luminous intensity

Luminous intensity is measured in candela and it projects the amount of light coming from a source in a particular solid angle. The luminous intensity is the function of point source and the direction of light source. It is the counterpart of radiant intensity and is the number of ray lines coming from a source, transmitted through the surface or reflected off the surface in a solid angle. It depicts the amount of power coming from a solid angle. [50]

$$lumens \tag{3.9}$$
$$= (radiant\ flux\ in\ watts)\ X\ \left(683\frac{lumen}{watt}\right) X\ (luminous\ efficiency)$$

Which can be written as,

$$I_v = 683\ \Phi_e\ V(\lambda) \tag{3.10}$$

3.3.4 Luminous flux density: Illuminance

Illuminance is the photometric irradiance [48]. It depicts the amount of radiant flux coming from, transmitted through or coming off the surface incident on the particular surface area with the weighted function of the human eye response at a specified wavelength. It is the radiant flux density as perceived by the human eye. Illuminance is measured in lux or lumen per square meter. The position of the surface at which the ray line is incident is an important factor for its precise perception with a human eye. [48]From the definition, illuminance can be represented as [49] :

$$\mathrm{E}_v = \frac{\Phi_v}{A} \tag{3.11}$$

where A is the area of the sphere. Substituting the value of luminous flux in the equation (X), illuminance can be written in lumen per square meter as [49]:

$$\mathrm{E}_v = \frac{\Phi_v}{A} = \frac{4\pi I}{4\pi R^2} = \frac{I}{R^2} \tag{3.12}$$

The equation concludes that illuminance is dependent function of intensity and the distance. It show inverse relation of illuminance with the square of the distance.

3.4 Luminance

Luminance is described as the flux lines passing from a point source in a particular point of a surface area in a specified direction over a solid angle. Luminance is the function of a point source, the direction of the flux lines from a point source, the direction of rays towards the stated surface, the point of the surface with an area and solid angle of the surface environment. It depicts the brightness of the specified surface and is defined by

candela per square meter or Lumen per square meter per steradian. Luminance is the quantity which explains the phenomenon of light passing or reflected of the specified surface and perceived by the human eye over the boundary of solid angle. The solid angle defines the number of flux lines reaching the human eye. Although the number of flux lines received is much less compared to the lines coming from the solid angle, it gives a valid argument of human perception of light. Correspondingly, the reception of flux lines depends on the diameter of an individual's eye under visions like photopic, scotopic and mesopic visions and the wavelength of the source. Luminance can be expressed as the ratio of luminous intensity and the area of the subtended surface. The definition can be represented as follows: [47]

$$\text{Luminance} = \frac{\text{Luminous Intensity}}{\text{Area}} \tag{3.13}$$

From the definition of illuminance and luminance, their relation can be depicted in candela per square meter as [49] :

$$\text{Luminance} = \frac{\text{Illuminance}}{\text{solid angle}} \tag{3.14}$$

Luminance can be depicted as follows by stating the values of luminous intensity and Area, [48]. Luminance is a dependent factor of intensity of the power source which defines the number of flux lines that reaches human eye through the solid angle subtended from the source.

$$\text{Luminance} = \frac{683\ P_t\ v(\lambda)}{4\pi R^2} \tag{3.15}$$

where p_t: Power of light source in watts, $v(\lambda)$: Spectral Sensitivity Function which provides the conversion between radiometric and photometric units, 683: Normalizing factor i.e. it converts watt into lumen (Lumen/watt), r: distance between source and receiver. Friis equation describes that the received power to transmit power ration is a dependent factor of the aperture area of transmitter and receiver. Luminance represents the dependency of flux lines coming from a solid angle of a sphere from a point or isotropic source. It shows that luminance is dependent on the aperture area of a source and does not include the aperture area of an eye. The luminance provides an approximate estimation of flux lines coming or reflected off the surface, but the number of flux lines received by an eye is much less compared to the amount of luminous flux coming from a solid angle. Thus, taking an analogy from the Friis equation, there is a need for the aperture area of an eye in the luminance equation to develop a precise path loss model in photometry. Taking into consideration, the aperture of an eye($\pi D^2/4$) in the above equation yields:

$$P_r = \frac{683\ P_t\ v(\lambda)\ \pi D^2}{4\pi R^2\ \ 4} \tag{3.16}$$

The aperture area of an eye provides a precise estimation of received number of lumens by human eye with the above equation.

4. PROPOSED SOLUTION

4.1 General

Electromagnetic radiation is the wave that propagates in space-time carrying electromagnetic energy [30]. The propagation of waves is identical for light and radio wave, but their behavior is characterized by the propagating wavelength. The wavelength discriminates all the waves in the EM spectrum and in consequence, the human eye cannot perceive them. Human eye senses the wavelength under the visible portion of the spectrum. Beyond this portion, a human eye is not sensitive to convert the waves to chemical and electrical energy for detection. In this thesis research, an attempt is made to associate radio wave with the visible light wave. A relationship is developed to estimate a medium to visualize the radio waves with a human eye. It is an empirical effort to convert the radio wave coming from Wi-Fi source into the light wave to make the radiation visible to our eye. As discussed in the previous chapter, the considered propagation model is based on free space loss and loss of wall. Thus, the correlation between the two waves is carried out in two phases. In the first phase, the relation is determined by using extended Friis equation of radio wave (4.3) and sophisticated model of photometric luminance (3.16) as discussed in chapter-3. The established relation of two concept defines the dependency of alpha with respect to loss of wall in addition to some constant. The instituted equation will define the transparency of a film represented by alpha α , with respect to loss of wall, L_w. The value of alpha is calculated with respect to corresponding loss of the wall on a linear scale and consequently all the value is normalized between 0 to 1 to outline the transparency of the film.

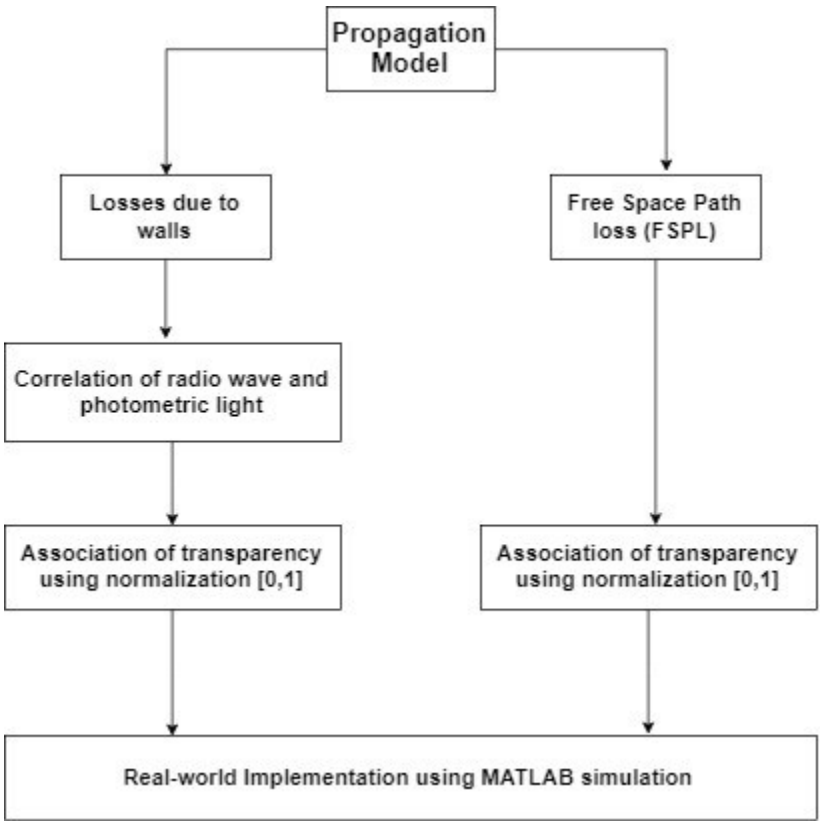

Figure 4.1 Flow-chart representation of proposed solution

Furthermore, the free space path loss (FSPL) is estimated by using the equation of free space path loss from Friis Equation. The free space path loss is considered for a maximum range of Wi-Fi at 2.4 GHz and 5 GHz in an indoor environment and thus, normalized between 0 to 1 to represent film characteristics. Accordingly, the total loss represents the transparency due to the wall and free space path loss. The path loss prediction of the propagation model is demonstrated using MATLAB simulations using an indoor digital map. The transmitter is represented by the transparency of FSPL, the walls are represented by corresponding transparency due to the wall and the receiver is

indicated by an image. The perception of the image at the receiver location from the transmitter depicts the accessibility of the Wi-Fi signal. The result provides a simulated reality of how this research might be utilized in a real-world scenario and helps to envision the radio wave interaction with the environment after implemented using augmented reality.

4.2 Inverse Square Law

The inverse square law is based on the fundamental concept of geometrical consideration. The geometrical concept illustrates that a point source emitting intensity in all direction has the tendency to lose its energy with the increase in distance. The definition states that the spread-out signal source is inversely proportional to the square of the distance from the source to the point on the specified surface [52]. The intensity of the source at a distance r from the specified quantity can be represented as:

$$I = \frac{P}{4\pi r^2} \tag{4.1}$$

Where, P = power of the source and $4\pi r^2$ is the area of the sphere.

Thus, intensity and distance relationship has been depicted by equation 4.2. The intensity decreases due to the spread of the signal over a large surface when the distance of the intensity of light increases from its source.

$$I \propto \frac{1}{r^2} \tag{4.2}$$

The total number of flux or ray lines are a dependent factor of the power of the source and is always constant over the distance of its influence [52]. The total surface area increases with the square of the distance from the source to destination and consequently, the limited flux lines get spread over the surface area. The number of flux lines on the specified surface defines the intensity level from the source as depicted in the figure below:

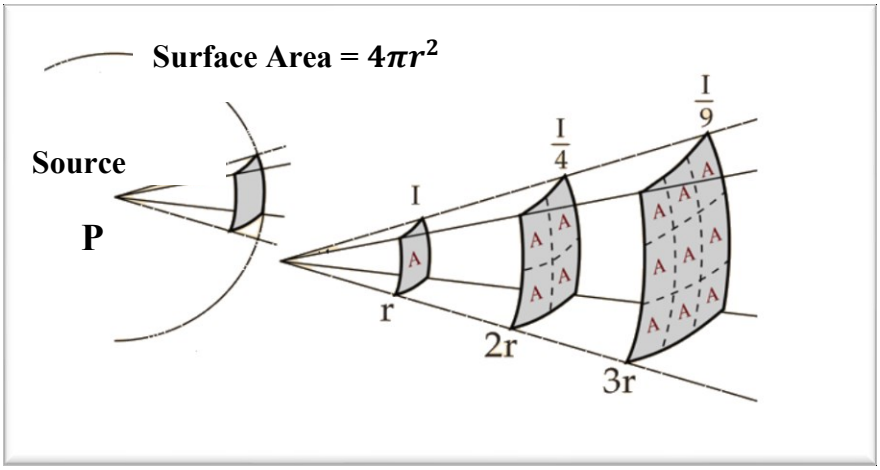

Figure 4.2 Inverse relation of Intensity with distance [50]

Figure 4.2 illustrates the geometric concept that the intensity of the source decreases by four as the distance is double due to its spread over the increased surface area. The figure depicts that the level of intensity is a dependent factor of the surface area of the subtended surface over which the intensity if incident and the level of the intensity transmitted from the source. The power defines the number of flux lines coming from the source in the direction of the incidence over the surface. The inverse square is equivalent for all the waves radiating in the space as they behave in the identical manner.

4.3 Correlation of Radio Wave and Photometric Light

4.3.1 Wi-Fi: Friis equation

Friis Equation is the fundamental concept in antenna theory to estimate the received power under free space environment. As discussed in chapter-3, the received power can be determined using formula 2.1. In this thesis, an empirical factor L_w is incorporated into the equation to include the loss of wall under the influence of free space environment. Presume if the losses between the two antennas are considered due to the n number of wall i.e. L_w, then the Friis equation can be represented as

$$P_R = \frac{P_T A_{effr} A_{efft}}{R^2} = \frac{P_T \lambda^2 {L_w}^n}{(4\pi R)^2} \tag{4.3}$$

where, $A_{eff} = \lambda/4\pi$ is the effective area.

The loss of wall will depend on the type of obstacle material like wood, glass, concrete, and brick for 2.4 GHz. The obstacle in the environment is considered as a homogeneous material with a defined loss.

4.3.2 Light

In photometry, the perception of a brightness of the human eye is achieved through luminosity function. The conversion from radiometric to photometric units is done using luminous efficiency function or eye sensitive function. At 555nm, the human eye is most sensitive and thus V(λ) is unity. Based on the luminosity function, the wavelength-weighted power emitted by a light source in a direction per unit solid angle is given by luminous intensity. The brightness of light can have a lot of meanings which is

understood using three concepts. The amount of light coming from a light source is called luminous flux measured as lumens. Similarly, the amount of light falling on a surface coming from a light source is called illuminance measured as lux. Conclusively, the amount of light reflected off a surface in a solid angle is called luminance measured in candela/meter square. However, received power of light is the receiver sensitivity of the human eye and expressed using equation (3.16). In this thesis, a heuristic variable α^n is included in the equation to define the transparency of the film. The variable is implemented to examine the experimental aspect of the transparency with path loss. The revised equation can be represented as below and is measured in Candela:

$$P_r = \frac{683\ P_t\ v(\lambda)\ \pi D^2 \alpha^n}{4\pi R^2\ \ 4} \tag{4.4}$$

Since both Friis equation and photometric light equation follow the inverse square law (4.2), it is assumed that the ratio of their output to input power is equal. From Equation 1 and 2, we have

$$\frac{P_R}{P_T}(wifi) = \frac{P_r}{P_t}(light) \tag{4.5}$$

Associating these equations, the relation between alpha and loss of wall can be defined as

$$\alpha = L_w . \sqrt[n]{\frac{k1}{k2}} \tag{4.6}$$

where,

$$k2 = (683\ V(\lambda)\ \pi\ D^2) \tag{4.7}$$

and

$$k1 = \frac{\lambda^2}{\pi} \tag{4.8}$$

The concluded relation between loss of thin film, α, and loss of wall, L_w represents the direct dependency of alpha with loss of wall with added constants from Friis equation under 2.4 GHz and photometric luminance under a monochromatic source at 555 nm. This relationship provides the basis for converting radio wave loss into light wave transparency. This relation of alpha and loss of wall is represented by :

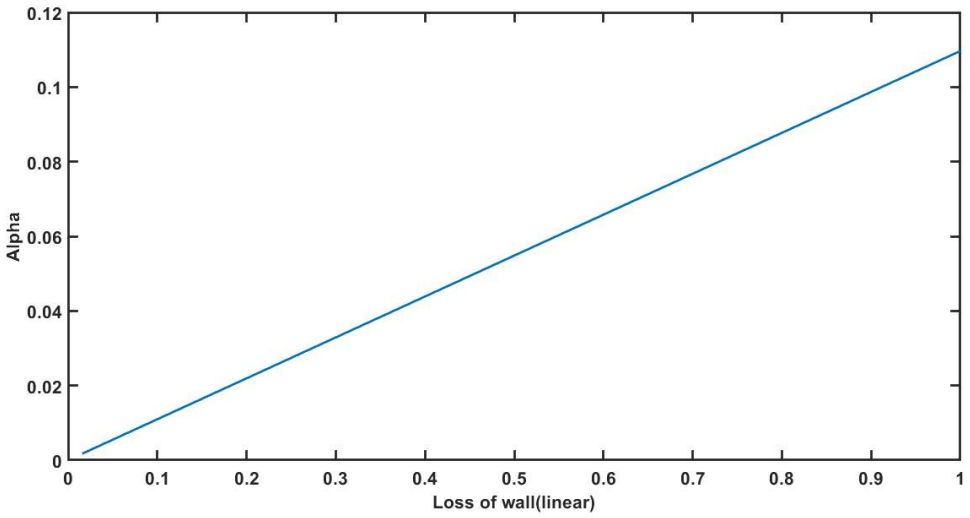

Figure 4.3 Graphical representation of Alpha with loss of wall

The graph in figure 4.3 represents the linear relation of alpha with loss of walls (linear value) including constants. The value of Alpha increases with increase in linear value of losses from a sample of -30 dB to 0 dB. The maximum value of alpha is depicted at 0 dB.

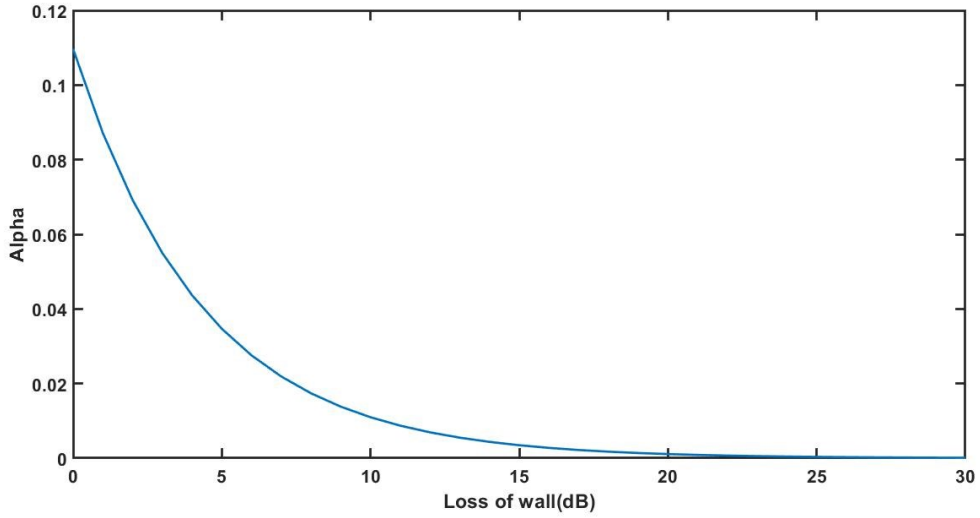

Figure 4.4 Graphical representation of Alpha with loss of wall

The relationship of alpha and loss of wall (dB) in figure 4.4 shows that the value of alpha decreases abruptly from 0 to -20 dB. The graph illustrates that alpha gradually decreases from -20 dB. Accordingly, the relation depicts an exponential decrease of loss of wall after this point .Under 2.4 GHz condition, the transparency values are estimated between 0 to 1 by normalization. The normalized values between for the range of L_w=1(0db) to L_w=0.016(-18 dB) is represented by the table 4.1. The value has been taken to observe the change of transparency value for the maximum signal attenuation provided by the concrete wall at 2.4 GHz. The attenuation is considered for the typical indoor environment conditions like office buildings, house , and warehouses. The figure 4.5 shows that transparency value shows a drastic increase of the loss till 10 dB and starts increasing after 10 dB. Thus, the transparency is affected with a small variation of the signal attenuation after this point.

Table 4.1 Transparency values due to loss of wall

linear value	loss (dB)	Alpha	Normalized Value
1.000	0	0.110	0.00
0.794	-1	0.087	0.21
0.631	-2	0.069	0.37
0.501	-3	0.055	0.51
0.398	-4	0.044	0.61
0.316	-5	0.035	0.69
0.251	-6	0.028	0.76
0.200	-7	0.022	0.81
0.158	-8	0.017	0.86
0.126	-9	0.014	0.89
0.100	-10	0.011	0.91
0.079	-11	0.009	0.94
0.063	-12	0.007	0.95
0.050	-13	0.005	0.97
0.040	-14	0.004	0.98
0.032	-15	0.003	0.98
0.025	-16	0.003	0.99
0.020	-17	0.002	1.00
0.016	-18	0.002	1.00

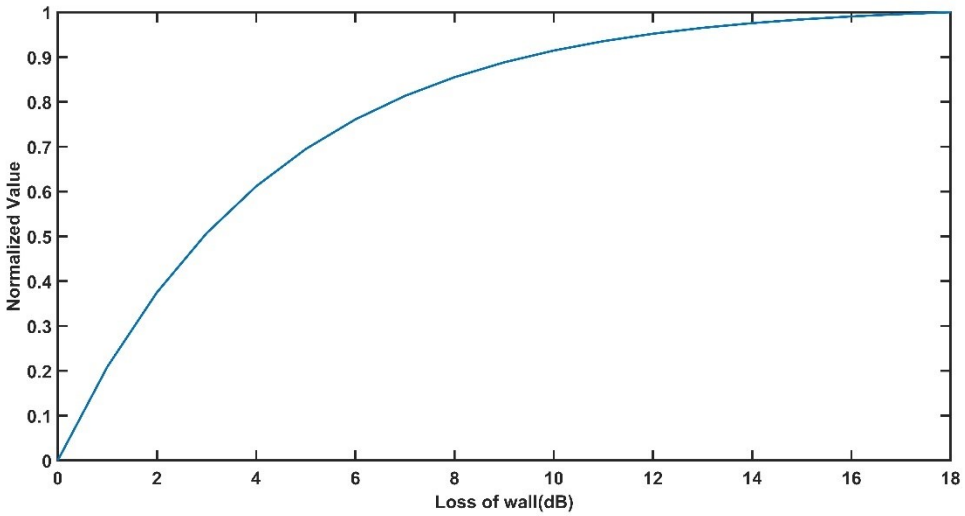

Figure 4.5 Relationship between transparency values with loss of wall

Similarly, the relationship of alpha with loss due to wall for 5 GHz is represented for a maximum loss of 30 dB accounted by a concrete wall. The figure 4.6 illustrates the the similar relation of gradual decrease of alpha after 10 dB as seen in 2.4 GHz. There is a very little effect of frequency on the value of alpha. The value of alpha has been normalized between 0 to 1 for a maximum range of 30 dB and is depicted in figure 4.7

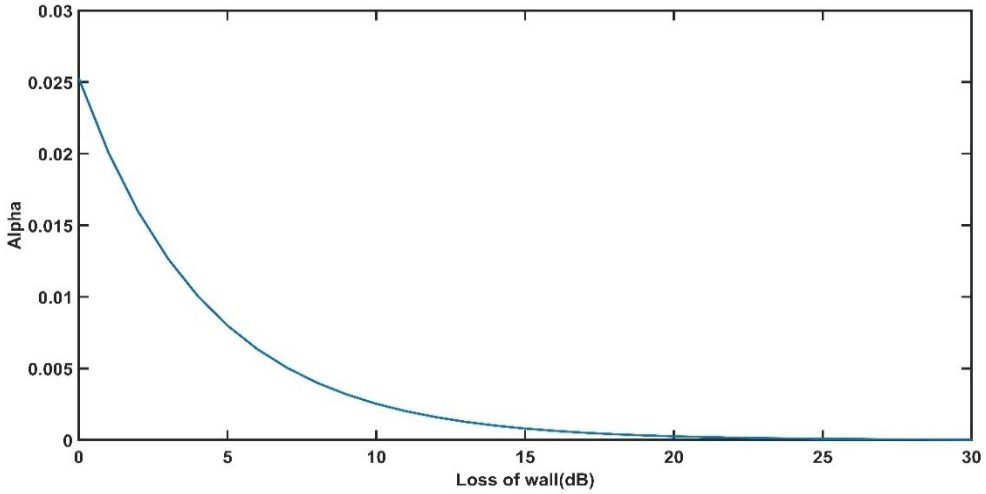

Figure 4.6 Relationship between Alpha with loss of wall (dB)

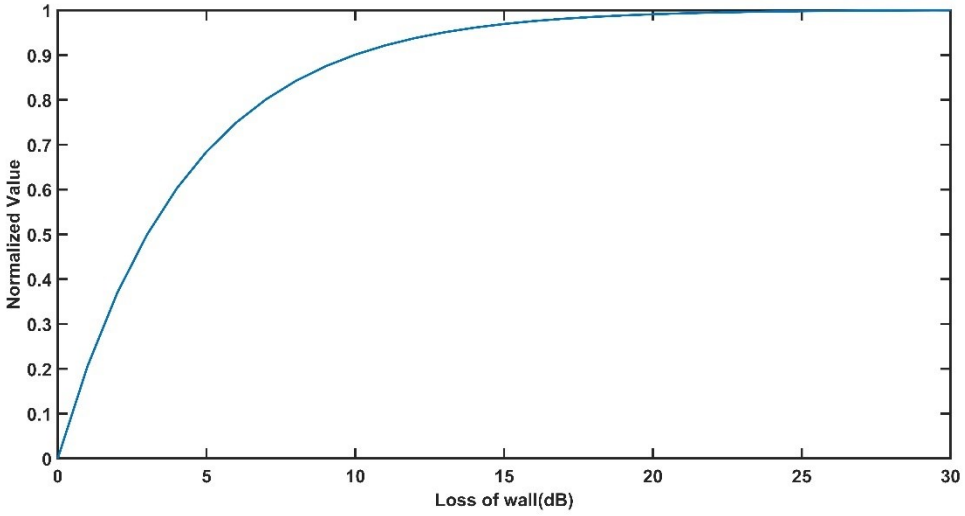

Figure 4.7 Relationship between normalized value with loss of wall

4.4 Free Space Path Loss

In this chapter, the relationship has been established between alpha and loss of wall. The consequent relation of the radio wave is determined to define the transparency of free space. In radio communication, Free space path loss is calculated using Friis Equation (2.1). The free space radio propagation occurs in the line of sight environment between transmitter and receiver. The free space loss of signal from the source is dependent on the aperture area and wavelength of the signal. The strength of the signal decreases with the increase in the square of the distance as per the inverse square law. Under this condition, there is a single path of radio propagation with no reflection and diffraction. Free space loss is expressed as [7]

$$FSPL = \left(\frac{4\,\pi Rf}{c}\right)^2 \tag{4.9}$$

λ is the signal wavelength (meters); f is the signal frequency (in hertz);R is the distance from the transmitter (meters), c is the speed of light in a vacuum. The equation of free space in dB form is given as

$$FSPL = 20log10(R) + 20log10(f) + 32.45 \tag{4.10}$$

where f measured in GHz and R measured in Km. A typical range of Wi-Fi (802.11n) under free space environment is 70 meters with the standardized signal quality for service requirement under 2.4 GHz [53]. In this thesis, the free space loss is calculated for the maximum distance of 70 meters. The result of the data set is normalized for a distance of 5 meters to 70 meters. The reference point is taken to be 5 meters as the free space loss is not affected below this distance range because the user is extremely close to the

transmitter. The normalization is from the concept of free space equation 4.11 which depicts that the loss is the function of the square of the distance and frequency. Thus, the normalized value for 2.4 GHz is calculated using the formula below

$$Normalization = \left(\frac{R}{5}\right)^{-2} \tag{4.11}$$

where, R=distance between transmitter and receiver (normalizing field) and 5 meters is the reference point. The table 4.2 depicts the normalized value that represents the transparency values of free space loss with distance under 2.4 GHz condition.

Table 4.2 Normalized Value of Free Space Loss

Distance	Free Space Loss(dB)	Linear Value of Loss	Normalized Value
5	-54.03	3.95037E-06	0.000
6	-55.62	2.74331E-06	0.307
7	-56.96	2.01549E-06	0.492
8	-58.12	1.54311E-06	0.613
9	-59.14	1.21925E-06	0.695
10	-60.05	9.87592E-07	0.754
11	-60.88	8.16192E-07	0.797
12	-61.64	6.85828E-07	0.831
13	-62.33	5.84374E-07	0.856
14	-62.98	5.03873E-07	0.877
15	-63.58	4.3893E-07	0.893
16	-64.14	3.85778E-07	0.907
17	-64.66	3.41727E-07	0.918
18	-65.16	3.04812E-07	0.928
19	-65.63	2.73571E-07	0.936
20	-66.07	2.46898E-07	0.942
21	-66.50	2.23944E-07	0.948
22	-66.90	2.04048E-07	0.953
23	-67.29	1.8669E-07	0.958
24	-67.66	1.71457E-07	0.962
25	-68.01	1.58015E-07	0.965
26	-68.35	1.46093E-07	0.968

Table 4.2 Continued			
27	-68.68	1.35472E-07	0.971
28	-69.00	1.25968E-07	0.973
29	-69.30	1.17431E-07	0.975
30	-69.60	1.09732E-07	0.977
31	-69.88	1.02767E-07	0.979
32	-70.16	9.64445E-08	0.981
33	-70.42	9.0688E-08	0.982
34	-70.68	8.54318E-08	0.983
35	-70.94	8.06197E-08	0.985
36	-71.18	7.62031E-08	0.986
37	-71.42	7.21397E-08	0.987
38	-71.65	6.83928E-08	0.988
39	-71.88	6.49304E-08	0.989
40	-72.10	6.17245E-08	0.989
41	-72.31	5.87503E-08	0.990
42	-72.52	5.59859E-08	0.991
43	-72.72	5.34122E-08	0.992
44	-72.92	5.1012E-08	0.992
45	-73.12	4.877E-08	0.993
46	-73.31	4.66726E-08	0.993
47	-73.50	4.47076E-08	0.994
48	-73.68	4.28642E-08	0.994
49	-73.86	4.11325E-08	0.995
50	-74.03	3.95037E-08	0.995
51	-74.21	3.79697E-08	0.995
52	-74.37	3.65234E-08	0.996
53	-74.54	3.51581E-08	0.996
54	-74.70	3.3868E-08	0.997
55	-74.86	3.26477E-08	0.997
56	-75.02	3.14921E-08	0.997
57	-75.17	3.03968E-08	0.997
58	-75.32	2.93577E-08	0.998
59	-75.47	2.83709E-08	0.998
60	-75.62	2.74331E-08	0.998
61	-75.76	2.6541E-08	0.998
62	-75.90	2.56918E-08	0.999
63	-76.04	2.48826E-08	0.999
64	-76.18	2.41111E-08	0.999
65	-76.31	2.3375E-08	0.999
66	-76.45	2.2672E-08	0.999
67	-76.58	2.20003E-08	1.000
68	-76.70	2.1358E-08	1.000

Table 4.2 Continued			
69	-76.83	2.07434E-08	1.000
70	-76.96	2.01549E-08	1.000
67	-76.58	2.20003E-08	1.000
68	-76.70	2.1358E-08	1.000
69	-76.83	2.07434E-08	1.000
70	-76.96	2.01549E-08	1.000

The relation of free space loss and normalized value with distance has been discussed for 2.4 GHz with different illustrations of graphs.

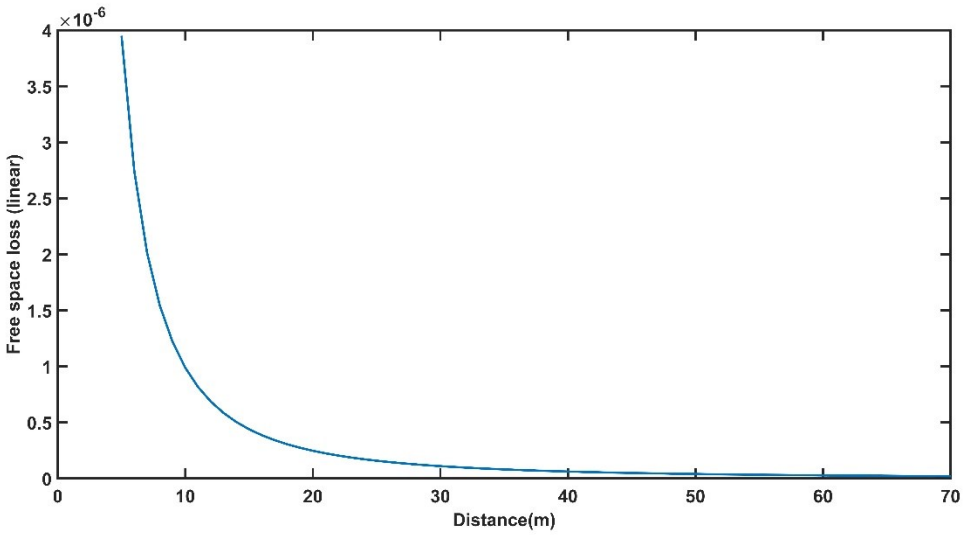

Figure 4.8 Relationship between free space loss (linear) with distance

Figure 4.8 represents the loss of free space with distance in meters. The free space loss has an abrupt decrease from 0 to 10 meters and starts decreasing gradually after this point. The linear value of the loss is decreasing exponentially with the distance.

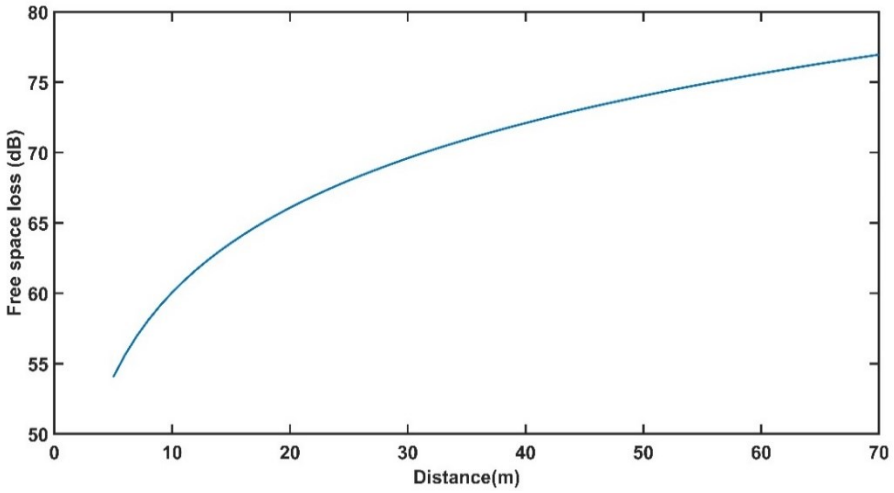

Figure 4.9 Illustration of relation of free space loss (dB) with distance at 2.4 GHz

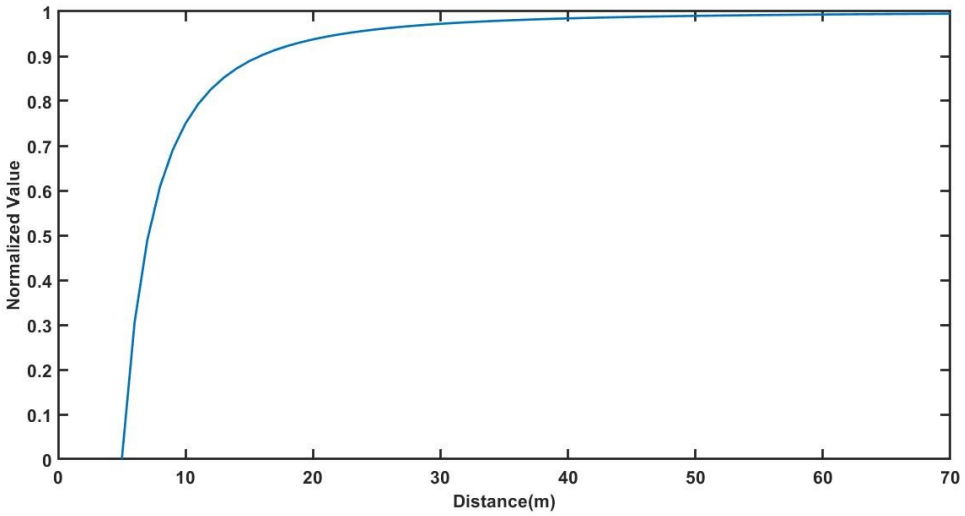

Figure 4.10 Illustration of relation of free space loss with distance at 2.4 GHz

The graph in figure 4.10 represents the same relation of Alpha with the loss of walls in dB. The graph illustrates the logarithmic association of loss with the distance in the free space environment. The association depicts the increase in the loss with the distance

under a typical indoor communication environment. Similarly, the normalization for 5 GHz has been done with respect to the 2.4 GHz. The normalization formula for 5 GHz is represented as follows :

$$Normalization = \left(\frac{R}{5}\right)^{-2} * \left(\frac{f2}{f1}\right)^{-2} \tag{4.12}$$

Where, $f2 = 5\ GHz$ and $f1 = 2.4\ GHz$.

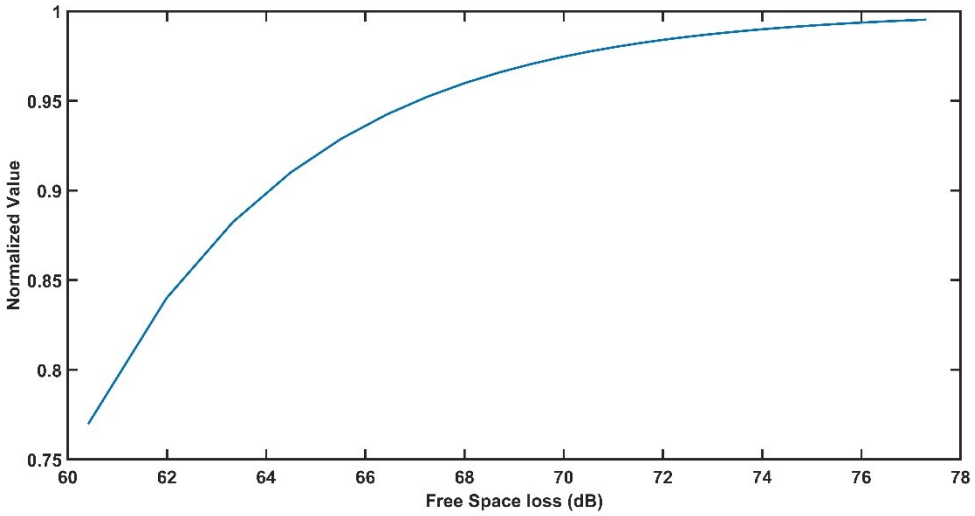

Figure 4.11 Illustration of relation of free space loss with normalized value at 5GHz

The normalization of 5 GHz has been done with respect to 2.4 GHz at a reference distance of 5 meters. Figure 4.11 and 4.12 illustrates the relation of normalized value with free space loss and distance respectively. The transparency value is relatively much

higher compared to 2.4 GHz at a distance of 5 meters. The change depicts the crucial dependency of frequency for the path loss prediction.

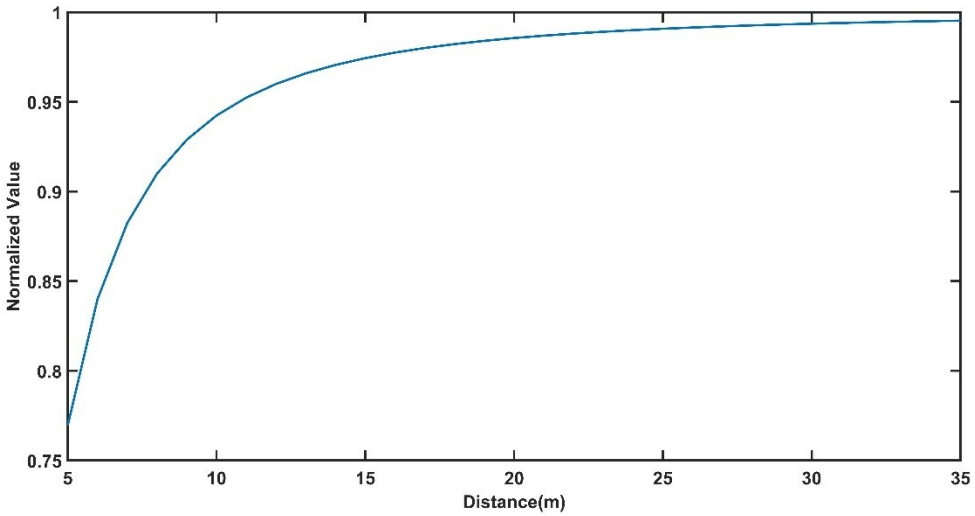

Figure 4.12 Illustration of normalized value with distance (m)

4.5 Film Characteristics Definition

The amount of flux lines that can pass through an object depends on the density of the material. The density of the material estimates the amount of light passing through an object. The material is characterized under three categories depending upon the light penetration and material's absorbing capabilities. The material is considered transparent when all the light passes through an object without any flux absorption. The light penetration level is 1 for this material. Consequently, when all the light flux is absorbed by the material and cannot pass over the material, it is termed as opaque material. The density of the material is maximum under these condition and light penetration is completely 0. When light penetration level is between 0 and 1, it is defined as translucent

material. Translucent behavior is characterized by an added combination of the penetration capability of a light source and the absorbing ability of the material. Under this condition, some level of light penetrates over the material and some flux lines are absorbed by the material unlike transparent and opaque. In this thesis paper, the characteristic of the material depends on the combined loss of free space and loss of wall. The normalized form of these losses represents the attributes of the film. The table depicts the characteristic of the film with respect to normalized value.

Table 4.3 Transparency characteristic of film

Attributes	Normalized Value
Transparency	0
Translucency	$0 < \alpha < 1$
Opaque	1

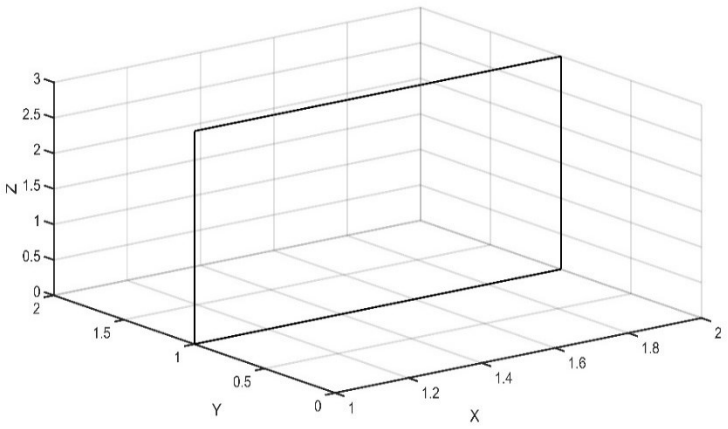

Figure 4.14 Illustration of film with transparency = 0

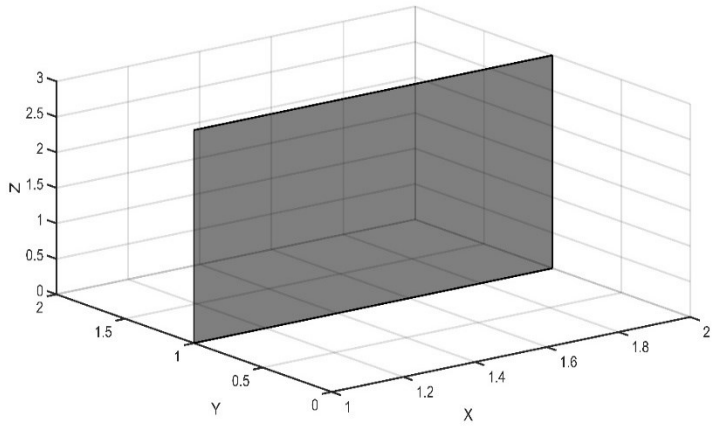

Figure 4.15 Illustration of film with transparency = 0.5

The total loss is represented by a variable α. Alpha is called the transparency factor. The reason for assuming this value range for alpha to comply with the MATLAB transparency definition standards.

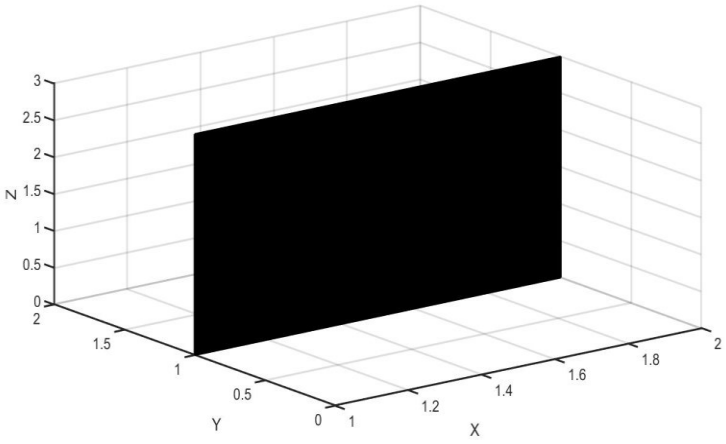

Figure 4.16 Illustration of film with transparency = 1

4.6 Proposed Algorithm

4.6.1 Plane-line intersection

An intersection of a line and a plane can be determined using geometrical and parametric concept. In three- dimensional space, a line either intersects the plane or lies inside the plane or there is no intersection [54]. When the line is parallel to the plane, it never intersects the plane while it may or may not intersect the plane if the line lies inside the plane. A line intersects a plane at a unique point when the line segment is neither parallel nor contained inside a plane. Let L be the line and Plane is denoted by P. A line segment with definite points P0 and P1 is represented by the following equation. [54]

$$P(s) = P0 + s(P1 - P0) = P0 + su \tag{4.13}$$

Where $u = P1 - P0$ is the direction vector of line, s is the real number and $P(s)$ is any point on the line segment P1P0 when $0 \leq s \leq 1$. When $s < 0$ or $s > 1$ the point $P(s)$lies outside the segment.

A plane P is defined by a point V0 and a normal vector n. Three cases are considered to determine the intersection of plane and line. First, it is checked whether the line segment is parallel to plane or not using the relation $n.u = 0$. If it holds true, the line segment never intersects the plane. The second process determines the disjoints of the line with the plane using relation $n.(P0 - V0) = 0$. It represents a point is contained in a plane P. The third process computes the intersection of line L with Plane P at a unique point $P(s_I)$. This intersection can be computed using the parametric equation below: [54]

$$s_I = \frac{-n.w}{n.u} = \frac{n.(V0 - P0)}{n.(P1 - P0)} \tag{4.14}$$

Where $w = (V0 - P0)$ and is equal to $n.(w + s.u) = 0$.

If $0 \leq s_I \leq 1$, the line segment intersects the plane at this point. This point represents the location of line and plane intersection. In this thesis, the discussed concept has been used to determine the number of walls intersected by a single ray coming from a source in the direction of the receiver using MATLAB. The code below illustrates the concept of calculating the intersection of the plane and line. The line segment is represented as a single ray of finite length between transmitter and receiver. The multi-patch GIS data contains planes like a glass window, wood doors, and concrete walls. These planes are represented by a coordinate system which defines their location and size on the complex environment. The line segment is also represented by a three-dimensional coordinate between transmitter and receiver. These coordinates are used to calculate the intersection point of a line segment with a total of 213 planes defined in the patch. The intersection point is defined using a MATLAB function *in-polygon*. The planes are defined as individual polygons and intersection of the line is depicted by using the function called *numel*. The MATLAB code for the calculation of intersection has been given below:

MATLAB CODE :

```
load('facet_IHU_Ground_Build.mat');
wall=facet_IHU_Ground_Build_A;
syms xI x y z y1 m n xx k mm;
m=1;
f=2400;
syms hitwall
hitwall=0;
prompt={'Enter x-coordinate for TX:',...
    'Enter y-coordinate for TX:',...
```

```
    'Enter z-coordinate for TX:',};
title ='Input Parameters';
answer=inputdlg(prompt,title);
X_coordinate_tx = str2double(answer{1});
Y_coordinate_tx = str2double(answer{2});
Z_coordinate_tx = str2double(answer{3});
%X_coordinate_rx = str2double(answer{4});
%Y_coordinate_rx = str2double(answer{5});
%Z_coordinate_rx = str2double(answer{6});
%equation of line%-----------------------------------------------
%P=[X_coordinate_tx Y_coordinate_tx Z_coordinate_tx];
%Q=[X_coordinate_rx Y_coordinate_rx Z_coordinate_rx];
X=[21]
Y=[5]
for NN=1
    xxx=0;
Xr=X(NN);
Yr=Y(NN);
P1=[X_coordinate_tx Y_coordinate_tx Z_coordinate_tx];
Q1=[Xr Yr 1];
distance = norm(P1 - Q1);
if distance<=0
    distance=1;
end
%equation of plane%-----------------------------------------------
a=1:213;
for i=1:length(a)
    Wi='Wall_';
    Wa=strcat(Wi,num2str(i));
    A=wall(i).position(1,1:3);
    B=wall(i).position(2,1:3);
    C=wall(i).position(3,1:3);
    D=wall(i).position(4,1:3);
    xv1=
[wall(i).position(1,1),wall(i).position(2,1),wall(i).position(3,1),wall(i).positio
n(4,1)];
yv1=
[wall(i).position(1,2),wall(i).position(2,2),wall(i).position(3,2),wall(i).positio
n(4,2)];
zv1=
[wall(i).position(1,3),wall(i).position(2,3),wall(i).position(3,3),wall(i).positio
n(4,3)
    AC=A-C;
    BD=B-D;
    mod_AC=sqrt(dot(AC,AC));
    mod_BD=sqrt(dot(BD,BD));
    n=cross(AC,BD)/(mod_AC*mod_BD);
        %Intersection of line and plane%--------------------------
    V0=A ; % and an arbitrary point that lies on the plane:
    I=[0 0 0] ;  %origin
    u = Q1-P1;
    w = P1 - V0;
    Ki = dot(n,u);
    Li = -dot(n,w);
```

```
sI = Ki / Li ;%compute the intersection parameter
Ii = P1+ sI.*u;
if (sI < 0 || sI > 1)
    check= 3;    %The intersection point  lies outside the segment, so there is no
elseif(isnan(sI) || sI == Inf || sI == -Inf)
        check=4;
    else
        check=1;
        xI(i)=Wa;
        y1=Ii;
xv=Ii(:,1);
xv2(i)=xv;
yv=Ii(:,2);
yv2(i)=yv;
zv=Ii(:,3);
zv2(i)=zv;
[in,on] = inpolygon(xv,yv,xv1,yv1);
caption = sprintf('Wall%d', i);
xx=numel(xv(on),yv(on));
  y=xI ~=0;
Intersected_walls= xI(y);
end
end
end
```

4.7 Propagation Model Implementation

The loss due to the wall is considered by counting the number of walls between the transmitter and receiver and consequently, assigning the signal attenuation corresponding to the wall type. The wall loss can be defined as follows:

$$Loss\ of\ wall = \sum_{i=1}^{l} K_{wi} L_{wi} \tag{4.15}$$

Thus, the total loss can be defined using multi-wall model in equation 4.16 where, L_{FS} is the free space path loss.

$$Total\ Loss = L_{FS} + \sum_{i=1}^{l} K_{wi} L_{wi} \tag{4.16}$$

5. RESULTS

5.1 Simulation Results for 2.4 GHz : General

The proposed propagation model is predicted using MATLAB simulation. The model is applied to five different scenarios for 2.4Ghz and four scenarios for 5 GHz with the various combination of free space and wall conditions. The scenarios are used to compare the transparency of the film under various indoor conditions and visualize the signal coverage with the perception of the human eye. Correspondingly, the heat map is simulated using MATLAB to present the signal strength distribution under complex indoor office environment. The heatmap depicts the signal strength from every possible view of the receiver.

The set-up is considered for free space condition where there is no wall and a free space environment with the combination of various walls between transmitter and receiver. Under perfect free space condition, the transparent film depicts the loss of free space path with no added loss of walls. The transparent film is placed at the transmitter location and an image is positioned on the receiver. An observer views the loss of free space by watching the image at the receiver under the influence of transparent film. The image appears to be crystal clear, translucent or completely dark depending upon the characteristic of the film. The situation under free space condition depends on the distance between source and recipient. Similarly, the second set-up which includes both wall loss and free space loss will encompass individual transparent film correspondingly. The film for free space is permanently positioned at the transmitter with

added transparency loss at each wall location. The observer views the image at the receiver under the affected loss of wall and free space. The characteristics of the film change with the normalized value between 0 to 1 as discussed in the previous section. The normalization was based on the factors affecting the individual losses.

5.1.1 Scenario-1

The first set-up is under perfect free space condition where there is no wall between transmitter and receiver. The considered distance between the source and destination is 6 meters. The film includes the transparency of free space loss at a distance of 6 meters. The normalized value for this scenario is 0.31 from table 5.1. The MATLAB simulation results under this condition are depicted in the table.

Table 5.1 Measurement result of scenario-1

Name	Value
Distance between TX and RX	6 meters
transparency due to FSPL	0.31
number of walls between TX and RX	0
Total loss	55.61 dB

The transparency alpha depicts the loss due to free space at the transmitter. The view of the image at the receiver location predicts the coverage and strength of the signal from the transmitter.

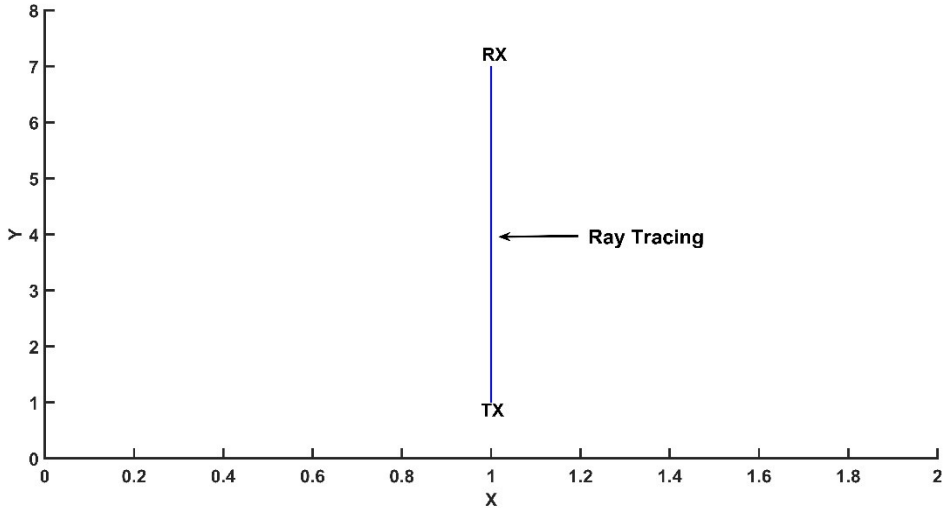

Figure 5.1 2D representation of scenario-1

In this case, the image is clearly visible to the human eye at a distance of 6 meters with the path loss of 55.61 dB. The transparency and signal level results describe that the signal level is easily accessible to the user for reliable connection of Wi-Fi services.

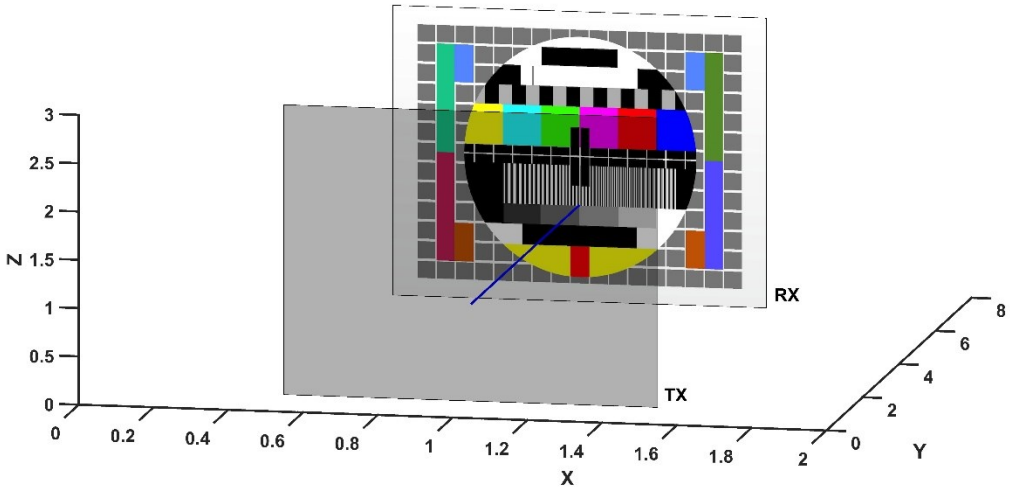

Figure 5.1 3D representation of scenario-1 with transparency of FSPL loss

5.1.2 Scenario-2

The scenario-2 is an extended form of the first set-up. The transmitter and receiver is under perfect free space condition with no wall, but the distance is considered to be 8 meters as depicted in figure 5.3. The total transparency under this condition is the free space loss of 58.11 dB. The Transparency value for this environment is 0.61. The MATLAB simulation results under this condition is depicted in table 5.2

Table 5.2 Measurement result of scenario-2

Name	Value
Distance between TX and RX	8 meters
transparency due to FSPL	0.61
number of walls between TX and RX	0
Total loss	58.11 dB

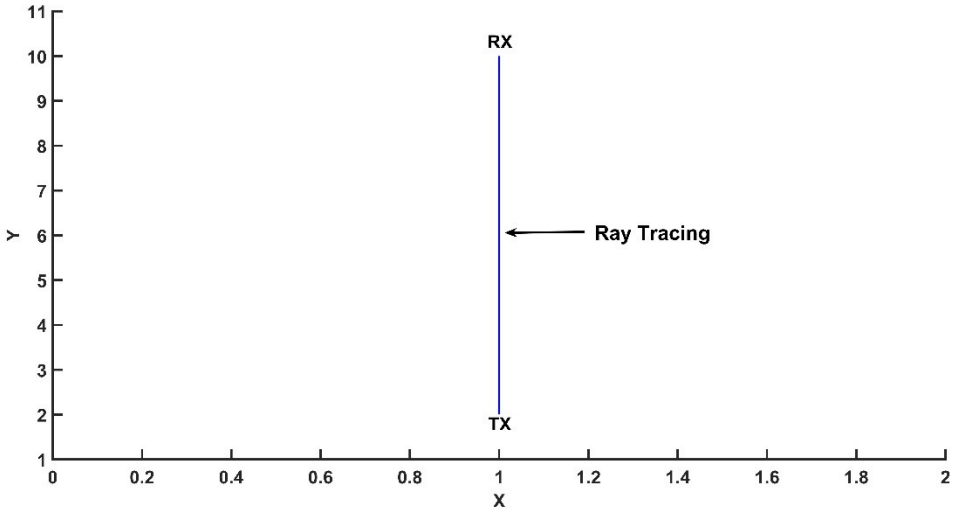

Figure 5.3 2D representation of scenario-2

The view of the image located at the receiver is under the influence of 0.61 transparency

and defines the loss of 0.39. The image is slightly vague compared to the first scenario and depicts the loss of signal with distance.

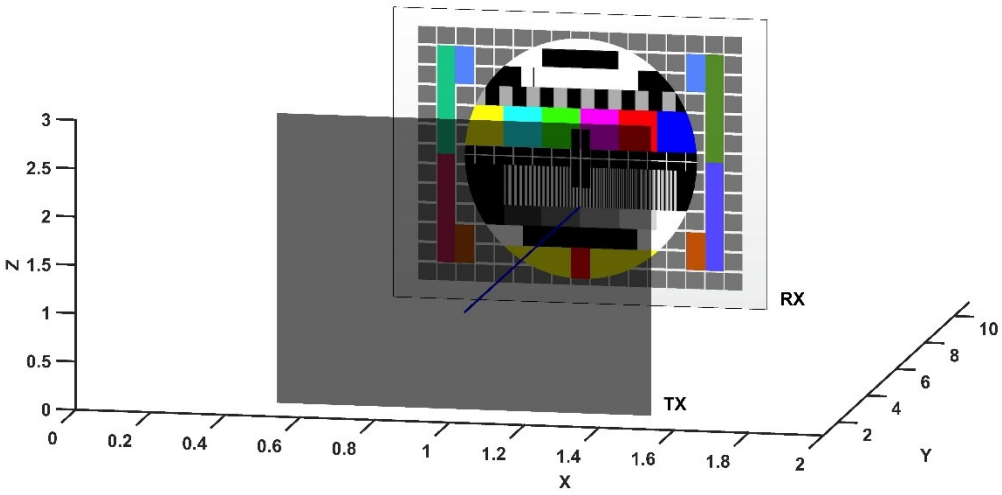

Figure 5.4 3D representation of scenario-2 with transparency of FSPL loss.

5.1.3 Scenario-3

Table 5.3 Measurement result of scenario-3

Name	Value
Distance between TX and RX	6 meters
loss due to FSPL	55.61 dB
transparency due to FSPL	0.31
number of walls between TX and RX	1
loss due to wall-1	2 dB
transparency due to wall	0.37
Total loss	57.61

The third scenario is a mixture of free space and a single wall between transmitter and receiver which is represented in fig 5.5.

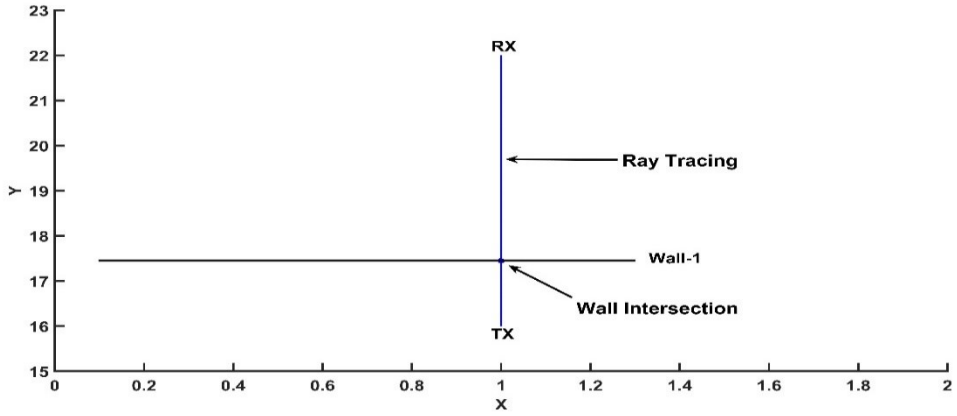

Figure 5.5 2D representation of scenario-3

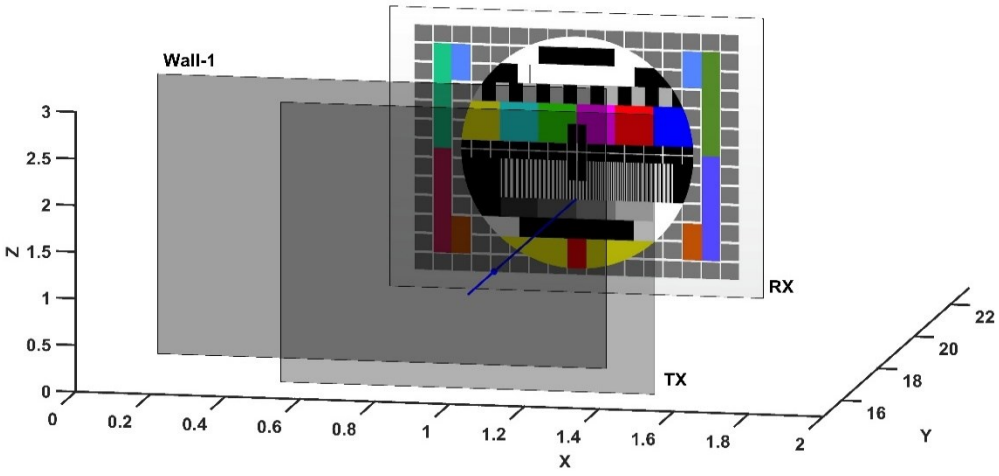

Figure 5.6 3D representation of scenario-3 with transparency of FSPL and wall loss

The considered distance between the source and destination is 6 meters and the normalized value for this loss is 0.31 from table 5.3. The loss due to wall-1 is considered

to be 2 dB and the corresponding transparency related to this loss is 0.37. The transparency due to the wall-1 is found to have a little effect on the total transparency as discussed in the previous section.

5.1.4 Scenario-4

Table 5.4 Measurement result of scenario-4

Name	Value
Distance between TX and RX	6 meters
loss due to wall-1	55.61 dB
transparency due to FSPL	0.31
number of walls between TX and RX	1
loss due to wall-1 and Wall-2	3 dB
transparency due to walls	0.5
Total loss	61.61 dB

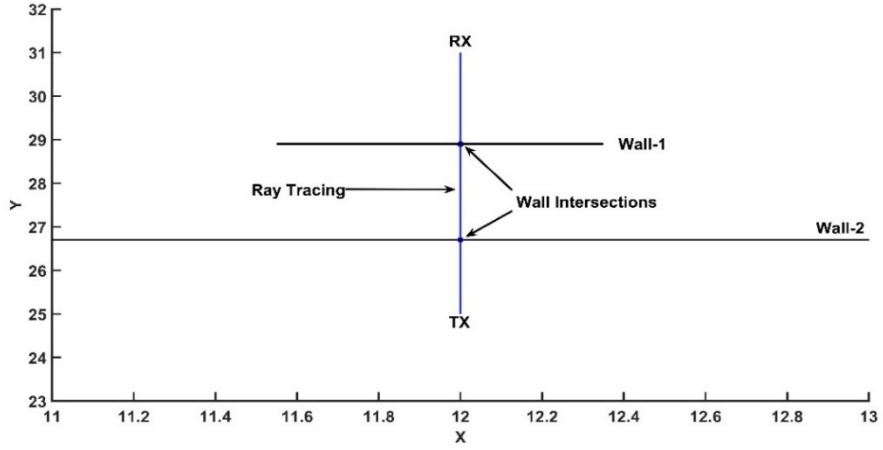

Figure 5.7 2D representation of scenario-4

The Fourth scenario includes free space distance and two walls between the transmitter and receiver. The considered distance between the source and destination is 6 meters. The

loss of each wall considered to be 3 dB. The MATLAB simulation results under this condition are depicted in the table.

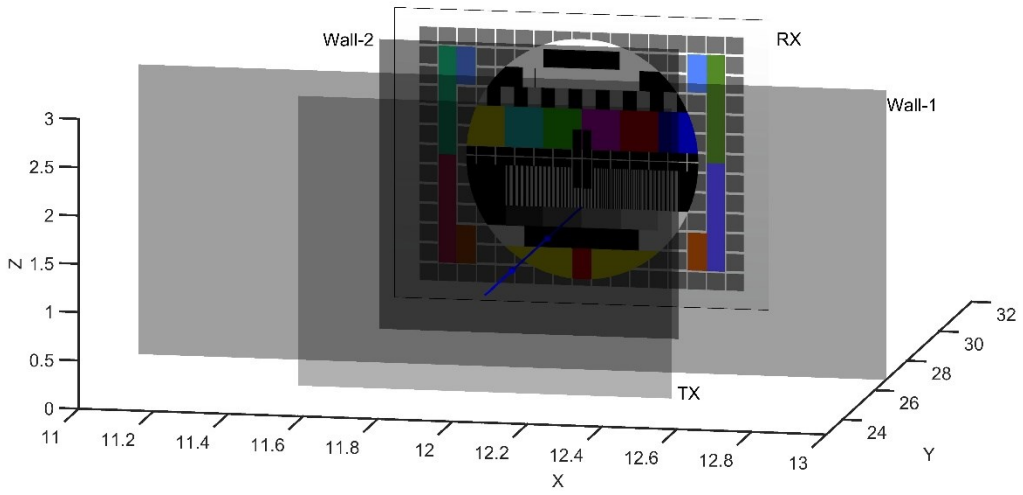

Figure 5.8 3D representation of scenario-4 with transparency of FSPL and wall loss

5.1.5 Scenario-5

The fifth scenario is the arrangement of free space and three walls between the transmitter and receiver. The considered distance between the source and destination is 6 meters. The loss due to wall-1 and wall-2 is considered to be 2 dB and the equivalent transparency related to this loss is 0.37 and correspondingly, wall-3 has a loss of 3 dB with the transparency of 0.5. The MATLAB simulation results under this condition are depicted in the table.

Table 5.5 Measurement result of scenario-5

Name	Value
Distance between TX and RX	6 meters
loss due to wall-1	55.61 dB
transparency due to FSPL	0.31
number of walls between TX and RX	3
loss due to wall-1 and Wall-2	2 dB
loss due to Wall-3	3 dB
transparency due to wall-1 and wall-2	0.37
transparency due to wall-3	0.5
Total loss	62.61 dB

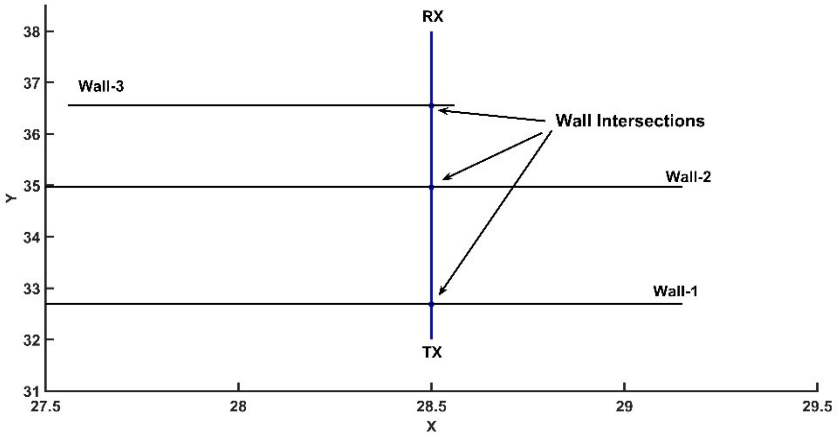

Figure 5.9 2D representation of scenario-5

The image is almost invisible from the transmitter. This depicts there is less coverage of signal in the current condition. The effect of three walls has dimmed the visibility of the colors in the image while the effect of the two walls has little effect on the signal coverage. This shows that a single wall can affect the coverage of signal in a huge amount due to the attenuation caused by the material construction.

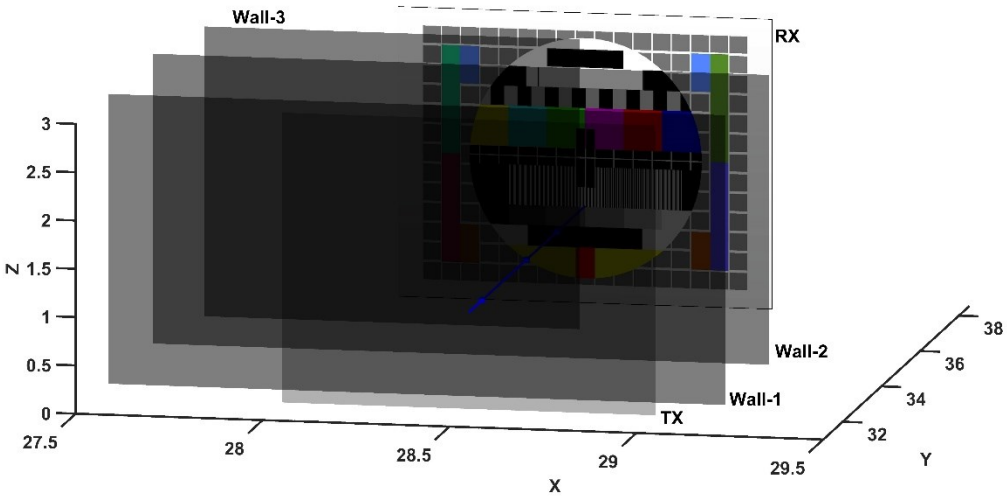

Figure 5.10 3D representation of scenario-4 with transparency of FSPL and wall loss

5.2 Simulation Results for 5 GHz

5.2.1 Scenario-1

Table 5.6 Measurement result of scenario-1

Name	Value
Distance between TX and RX	6 meters
transparency due to FSPL	0.84
number of walls between TX and RX	0
Total loss	61.99 dB

The first set-up is under perfect free space condition where there is no wall between transmitter and receiver. The considered distance between the source and destination is 6 meters. The film includes the transparency of free space loss at a distance of 6 meters.

The normalized value for this scenario is 0.84. The MATLAB simulation results under this condition are depicted in the table 5.6.

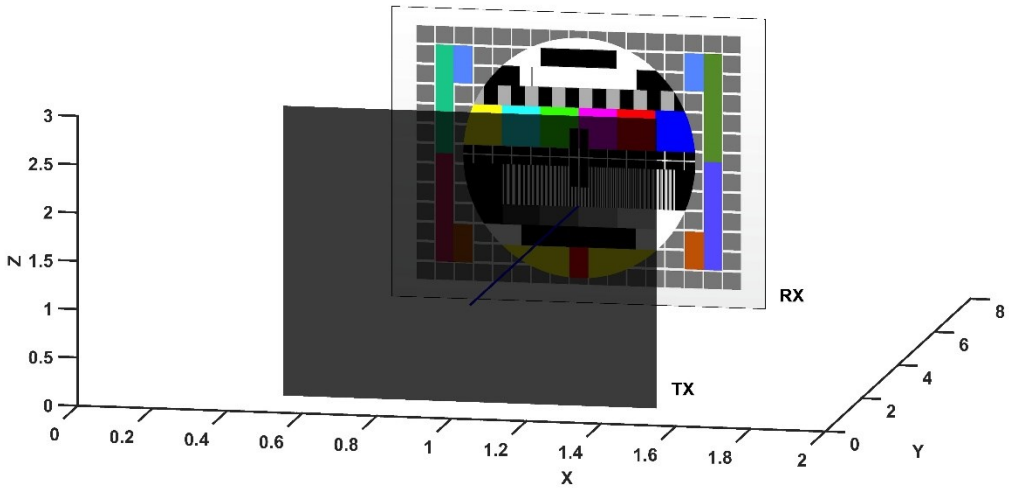

Figure 5.11 3D representation of scenario-1

5.2.2 Scenario-2

Table 5.7 Measurement result of scenario-2

Name	Value
Distance between TX and RX	7 meters
transparency due to FSPL	0.88
number of walls between TX and RX	0
Total loss	63.33 dB

The transmitter and receiver is under perfect free space condition with no wall, but the distance is considered to be 7 meters as depicted in figure 5.12. The total transparency

under this condition is the free space loss of 63.33 dB. The Transparency value for this environment is 0.88. The MATLAB simulation results under this condition is depicted in the table 5.7.

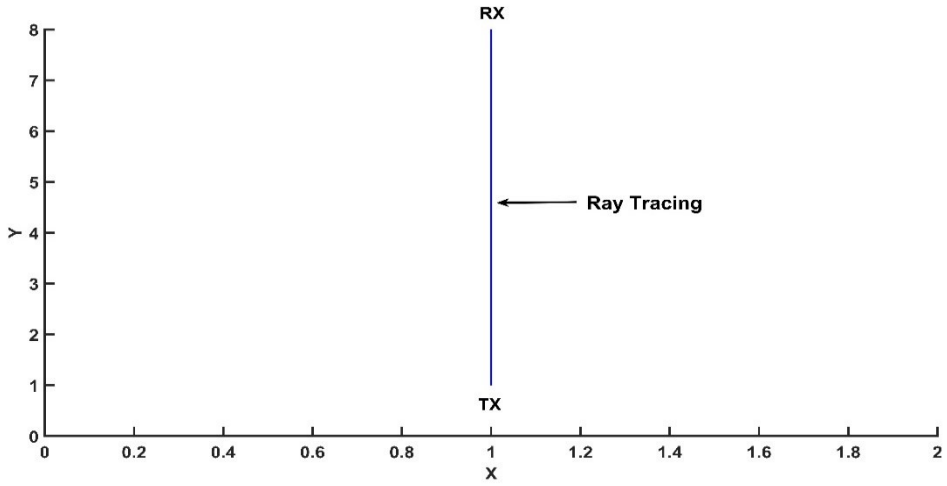

Figure 5.12 2D representation of scenario-2

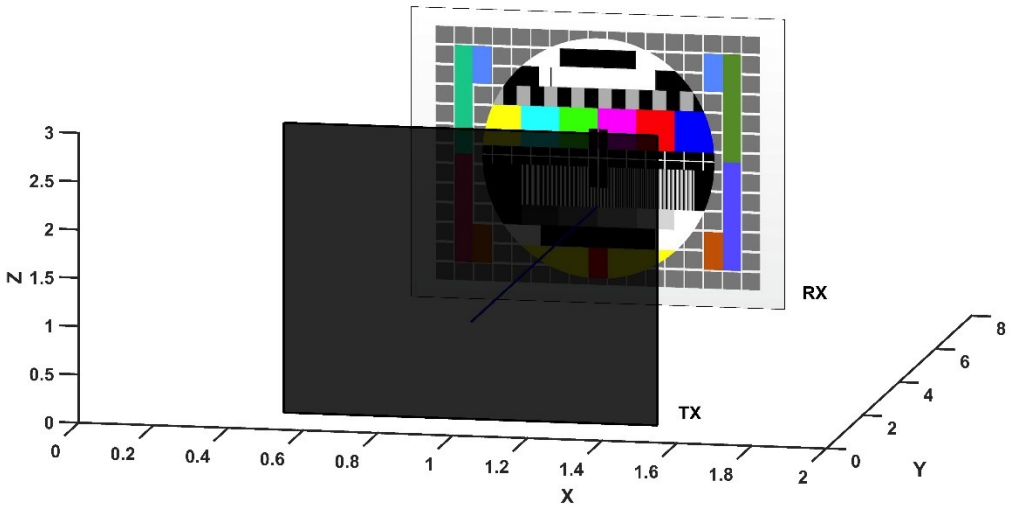

Figure 5.13 3D representation of scenario-2

5.2.3 Scenario-3

Table 5.8 Measurement result of scenario-3

Name	Value
Distance between TX and RX	6 meters
loss due to FSPL	61.99 dB
transparency due to FSPL	0.84
number of walls between TX and RX	1
loss due to wall-1	2 dB
transparency due to wall	0.36
Total loss	63.99 dB

The third scenario is a mixture of free space and a single wall between transmitter and receiver which is represented in fig 5.14.The MATLAB simulation results under this condition are depicted in the table 5.8.

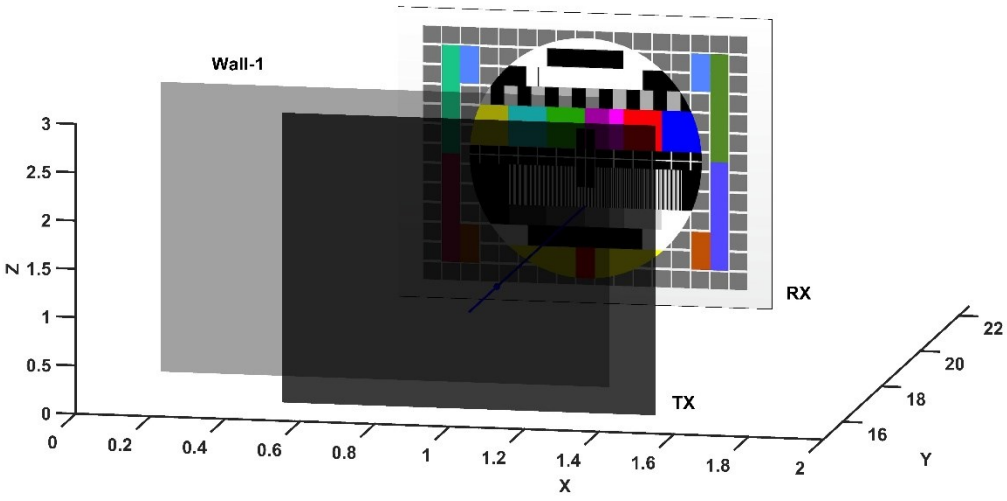

Figure 5.14 3D representation of scenario-3

5.2.4 Scenario-4

Table 5.9 Measurement result of scenario-4

Name	Value
Distance between TX and RX	6 meters
loss due to wall-1	61.99 dB
transparency due to FSPL	0.84
number of walls between TX and RX	2
loss due to wall-1 and Wall-2	3 dB
transparency due to walls	0.49
Total loss	67.99 dB

The Fourth scenario includes free space distance and two walls between transmitter and receiver. The considered distance between the source and destination is 6 meters. The loss of each wall considered to be 3 dB .The MATLAB simulation results under this condition are depicted in the table.

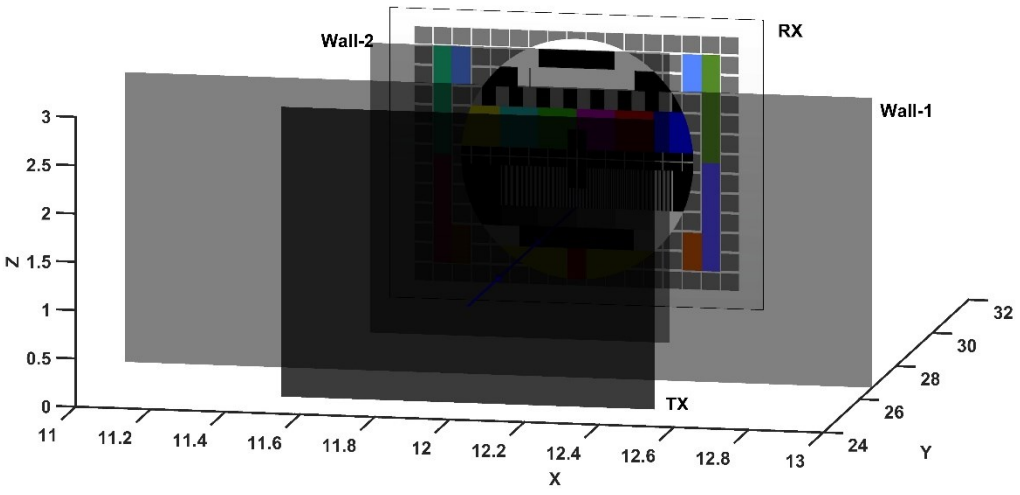

Figure 5.15 3D representation of scenario-4

6. RENDERING

This section describes the implementation of thesis research in an indoor building a vector map. The indoor vector map consists of partition materials like wood, glass , brick/concrete wall. The dielectric of these materials defines the level of signal attenuation and the attenuation is depicted by the film with different transparent values. The ray tracing method uses a ray technique to estimate the number of partition material between transmitter and receiver. The algorithm to trace the objects is based on the simple geometry of intersection of the line with the plane. The line is represented by a ray and the plane is illustrated as partition objects. Let us see the implementation of this thesis in an indoor environment with different in-building conditions. The measurements are done at the frequency of 2.4 GHz.

6.1 Two-Wall Scenario (Same Material)

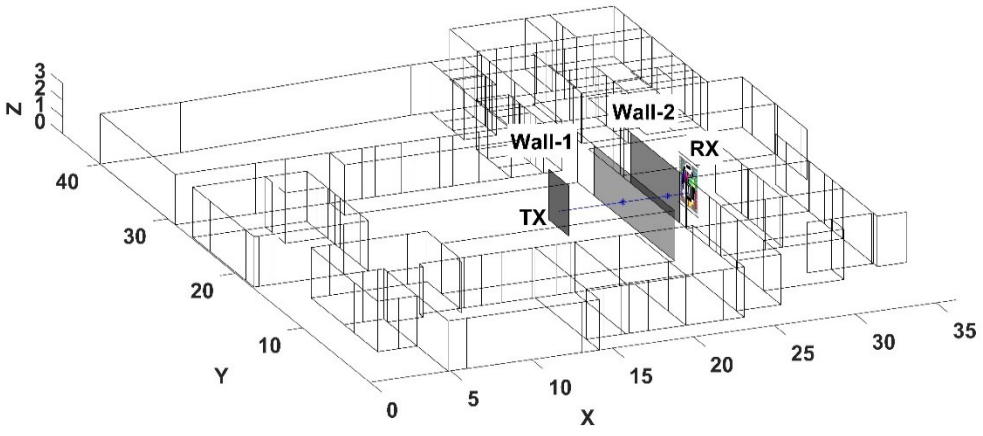

Figure 6.1 Ray tracing in an indoor vector map with same wall type

In this scenario, the distance between transmitter and receiver is 8 meters as depicted in figure 6.1. The ray traces the objects within this distance and finds two intersecting walls as defined as wall-1 and wall-2. The frequency used in the scenario is 2.4 GHz and the constitutive material losses are considered for the same frequency. The loss considered for both the walls are 2 dB and corresponding transparency for these losses are 0.3. The transparent film at TX location represents the FSPL loss for 8 meters and transparency related to this distance is 0.61. The image at RX location represents the reference of the Wi-Fi location. It provides a visual representation of how a Wi-Fi coverage would look at a distance of 8meters and two walls. It is represented by figure 6.2 which provides the front view of the same scenario as shown in figure 6.1.

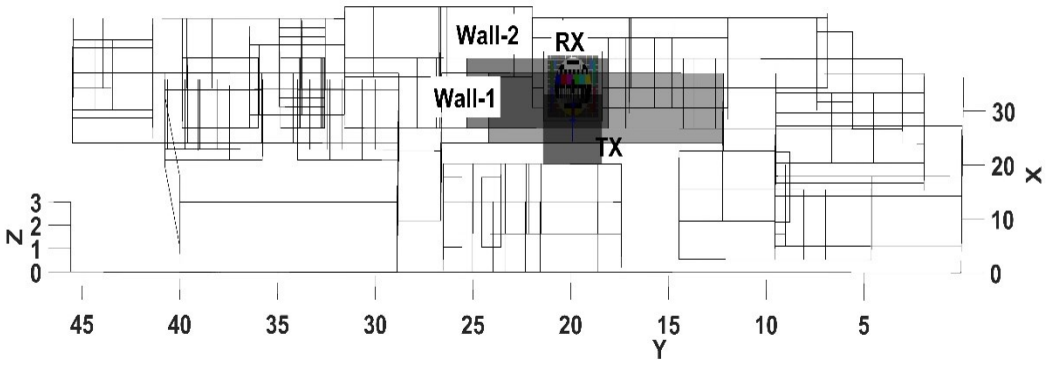

Figure 6.2 Front-view representation of the two-wall scenario

6.2 Two-Wall Scenario (Different Materials)

In this scenario, the distance between transmitter and receiver is 10 meters as depicted in figure 6.3. The ray traces the objects within this distance and finds two intersecting objects, door, and cubical wall. The loss considered for door and wall is 3 dB and 5 dB correspondingly. The comparison of two scenarios provides the computing capability of algorithm in a complex environment.

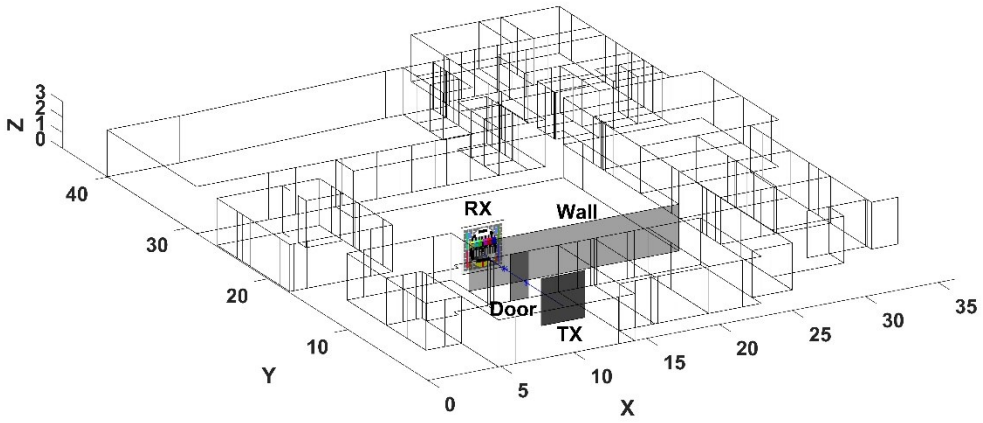

Figure 6.3 Ray tracing in an indoor vector map with two different walls

In comparison to the first scenario, the loss is greater for both free space and individual walls. The loss has increased the transparency values of both the factors and depicts the amount of signal loss on the way. The attenuation of the signal of signal depicts the amount of visibility of the image at RX location. The visibility of the image at Rx location has decreased with these increased losses as depicted in figure 6.4

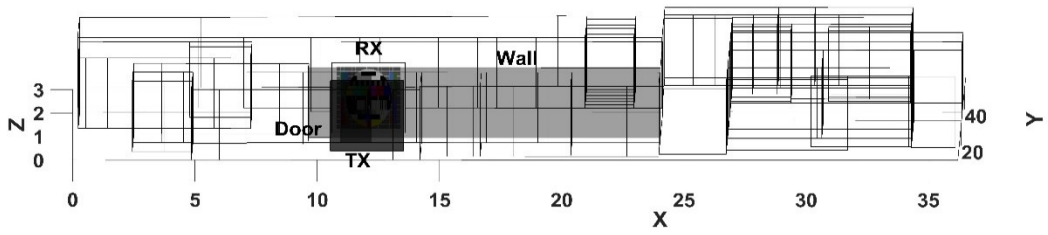

Figure 6.4 Front-view of an indoor vector map with two different walls

6.3 Three-Wall Scenario

In the third scenario, the distance between transmitter and receiver is 8 meters as depicted in figure 6.5. The ray traces the objects within this distance and finds three intersecting objects which are door ,window and typical ply wall. The loss considered for door, window, and wall is 3 dB and 3 dB, 5 dB correspondingly. A shown in figure 6.5, the visibility has completely decreased with the loss of three walls although the distance is similar to the first two scenarios. The signal attenuates due to the objects in the close distance with each other for a such a distance of 8 meters. The propagation of signal is affected by the dielectric of the material used for the construction of these walls. There is a drastic change of the visibility of the image in comparison two the first two scenarios. The signal coverage is completely affected and can be seen from figure 6.6. The location of transmitter and receiver is close to the obstructing objects which suggest that the signal has better signal coverage in comparison to the first two scenarios.

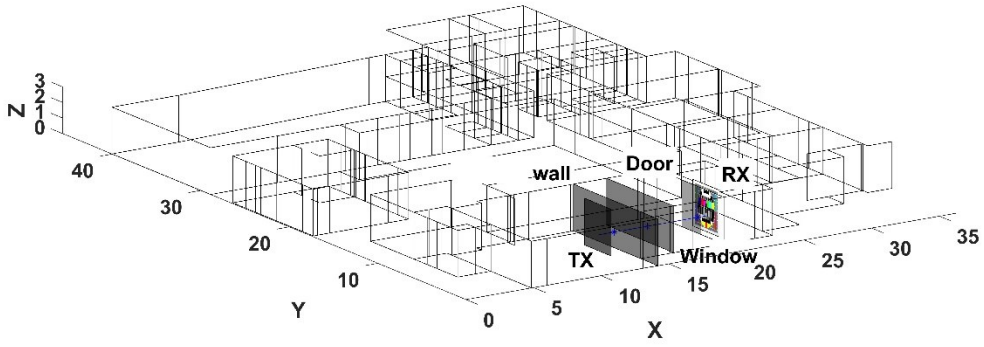

Figure 6.5 Ray tracing in an indoor vector map with three different walls

There is a drastic change of the visibility of the image in comparison two the first two scenarios. The signal coverage is completely affected as depicted by figure 6.6.

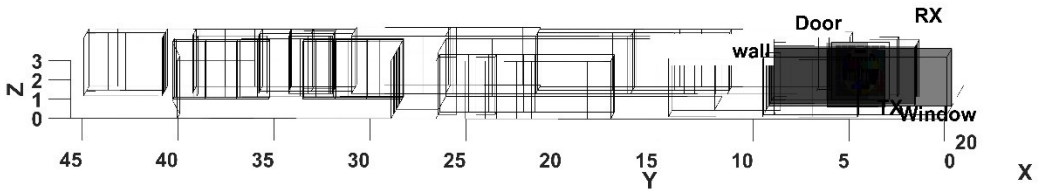

Figure 6.6 Front-view of an indoor vector map with two different walls

7. CONCLUSION

The indoor wireless communication has been growing rapidly in recent years due to the rise of a large number of subscribers that reside inside the buildings. The abrupt increase in the user has demanded the need for high signal penetration, seamless coverage, and high data throughput. To account all these factors, a high detailed analysis of the system deployment is needed. Thus, planning and optimization of an indoor network become a complex, time-consuming, and costly process. This thesis paper explores on providing the solution for all these problems by deploying radio propagation loss with the transparent film Characteristics. The visualization of radio wave losses provides a better understanding of the indoor propagation condition from both the operator and user's perspective and accordingly, assists in improving the signal coverage.

Chapter 2 discusses different propagation aspects of radio waves. The radio wave gets reflected, diffracted, and scattered while propagating from transmitter to receiver. These characteristics cause multipath of the signal and consequently, causes interference and fading. The propagation of signal is widely affected by the materials used in the building like a wood door, glass window, concrete/brick wall, cluster walls and many more. The dielectric of the material defines the level of signal attenuation caused in the path. To account all these problems, there are empirical models which estimate the path loss of radio waves using experimental measurements. It is not site-specific which makes it applicable in multiple scenarios, but it doesn't provide the precise measurement results. Thus, there are deterministic models which take into account all the propagation mechanisms accurately for a defined setup of an indoor system. But, the deterministic

models require a large database management and proper data collection for precise results. Both models provide certain advantages and disadvantages which has necessitated this thesis to combine the features of both models using the multi-wall empirical model to account the losses of walls and deterministic ray tracing algorithm for estimating the number of objects between transmitter and receiver.

Chapter 3 provides an introduction of light waves using radiometry and photometry. The radiometry is the measure of light wave propagation in space while the photometry is the subset of radiometry for the measurement of light with respect to the response of the human eye. This thesis explores the concept of photometry in order to convert the radio wave losses into photometric light transparency values. Taking, the analogy with radio wave communication, it has been assumed that photometric light propagation is similar except the fact that they have different wavelengths.

Chapter 4 provides an insight on the proposed solution to convert the radio wave losses with transparent film characteristics. To define the transparency for losses due to the walls, the concept of the inverse square has been considered for correlation. The inverse square law suggests that a point source radiating light or radio waves, it has a tendency to lose its energy with the distance due to the spreading of the signal over a large surface area. This analogy has provided the basis for correlating the radio wave and photometric light wave with the assumption that both the ratio of received power to transmit power of both the waves must be equal. This thesis has also included some heuristic factors like losses due to the number of walls and transparency film characteristics in radio and light

equations correspondingly. The correlation provides a relation of alpha with the losses due to the walls. This developed conversion formula is defined with the transparent film characteristics by normalizing the value of alpha for the maximum loss of 30 dB. Consequently, the transparency for free space path loss is estimated using the typical Wi-Fi range for indoor environment condition at different frequencies. The characteristic of the film is depicted by the normalized value of free space loss between the minimum and maximum loss accounted on the system. Thus, there are two different films for the representation of radio waves losses between transmitter and receiver. The combined transparency provided by these frequencies defines the total path loss permitted by the system.

Thus, this research is the novel work that provides a simpler and better understanding of indoor losses with visualization using transparent films. The propagation of wave and light behave in a similar manner which has assisted in finding the analogy relating them with respect to the sensitivity of the eye. Designing a propagation model using the analogy has developed a better understanding in evaluating the transmission of a radio wave in an indoor environment. A proper evaluation of signal strength provides better signal quality which positively improves the user experience in the network. This precise propagation mechanism would considerably simplify planning and troubleshooting of indoor Wi-Fi system in real-life using AR application. Hence, this research helps to have a better understanding of the network in a complex environment through visualization and provide a necessary prospect in improving the propagation modeling in future research.

8. FUTURE WORK

This thesis developed a transparency relation of the radio wave with the photometric light using propagation characteristics like free space path loss and loss due to the wall. However, there are some challenges on how to define the transparency with the total loss and can be accounted with future research work. Also, there is a need for characterization of many propagation mechanisms like reflection, diffraction, scattering which causes multipath, delay spread, power delay, coherence time, doppler effect and many more. The conversion of the radio wave to the light wave provided a basis for developing a transparency relation to visualize radio wave. This relation can be utilized with other propagation characteristic to develop a new transparency. These propagation characteristics will help to improve the path loss calculations in an indoor system and the interpretation of radio waves can be made precise. The proper modeling of the propagation model will provide a better visual understanding of the radio wave coverage. The network planners can exploit the application to design an indoor wireless system with minimum time and resource. The planning and optimization procedure can be made much simpler with the use of site-specific visualization of the radio wave. This thesis explores the behavior of signal in a typical indoor scenario of 900MHz, 2.4 GHz, and 5 GHz. A deep research is needed for indoor systems at other frequencies. Accordingly, this correlation can be studied for outdoor wireless systems like GSM, UMTS, LTE, and 5G networks. This research can be implemented with the AR scans which results in a vector map by scanning the indoor environment systems. Consequently, the transparent film depicting the radio losses provides a real-time analysis of indoor coverage with the help of AR scans.

APPENDIX SECTION

```
load('facet_IHU_Ground_Build.mat');
wall=facet_IHU_Ground_Build_A;
syms xI x y z y1 m n xx k mm;
m=1;
f=5000;
syms hitwall
hitwall=0;
prompt={'Enter x-coordinate for TX:',...
    'Enter y-coordinate for TX:',...
    'Enter z-coordinate for TX:',};
title ='Input Parameters';
answer=inputdlg(prompt,title);
X_coordinate_tx = str2double(answer{1});
Y_coordinate_tx = str2double(answer{2});
Z_coordinate_tx = str2double(answer{3});
%X_coordinate_rx = str2double(answer{4});
%Y_coordinate_rx = str2double(answer{5});
%Z_coordinate_rx = str2double(answer{6});
%equation of line%-----------------------------------------------
%P=[X_coordinate_tx Y_coordinate_tx Z_coordinate_tx];
%Q=[X_coordinate_rx Y_coordinate_rx Z_coordinate_rx];
%PQ=Q-P;
%[X,Y]=meshgrid(1:1:6,1:1:6)
X=[12]
Y=[31]
for NN=1
    xxx=0;
Xr=X(NN);
Yr=Y(NN);
P1=[X_coordinate_tx Y_coordinate_tx Z_coordinate_tx];
Q1=[Xr Yr 1];
distance = norm(P1 - Q1);
if distance<=0
    distance=1;
end
%equation of plane%-----------------------------------------------
a=1:213;
for i=1:length(a)
    Wi='Wall_';
    Wa=strcat(Wi,num2str(i));
    A=wall(i).position(1,1:3);
    B=wall(i).position(2,1:3);
    C=wall(i).position(3,1:3);
    D=wall(i).position(4,1:3);
    xv1=
[wall(i).position(1,1),wall(i).position(2,1),wall(i).position(3,1),wall(i).positio
n(4,1)];
yv1=
[wall(i).position(1,2),wall(i).position(2,2),wall(i).position(3,2),wall(i).positio
n(4,2)];
```

```
zv1=
[wall(i).position(1,3),wall(i).position(2,3),wall(i).position(3,3),wall(i).positio
n(4,3)];
%caption = sprintf('Wall_%d', i);
%text(xv1,yv1,zv1,caption)
    AC=A-C;
    BD=B-D;
    mod_AC=sqrt(dot(AC,AC));
    mod_BD=sqrt(dot(BD,BD));
    n=cross(AC,BD)/(mod_AC*mod_BD);
    %Intersection of line and plane%--------------------------
    V0=A ; % and an arbitrary point that lies on the plane:
    I=[0 0 0] ;  %origin
    u = Q1-P1;
    w = P1 - V0;
    Ki = dot(n,u);
    Li = -dot(n,w);
sI = Ki / Li ;%compute the intersection parameter
Ii = P1+ sI.*u;
if (sI < 0 || sI > 1)
    check= 3;    %The intersection point lies outside the segment, so there is no
intersection
elseif(isnan(sI) || sI == Inf || sI == -Inf)
        check=4;
   else
        check=1;
        xI(i)=Wa;
        y1=Ii;
xv=Ii(:,1);
xv2(i)=xv;
yv=Ii(:,2);
yv2(i)=yv;
zv=Ii(:,3);
zv2(i)=zv;
[in,on] = inpolygon(xv,yv,xv1,yv1);
caption = sprintf('Wall%d', i);
xx=numel(xv(on),yv(on));
  y=xI ~=0;
Intersected_walls= xI(y);
if xx==1
    xxx=1;
    hitwall=xI(i);
   ontheedge(m)=hitwall;
    m=m+1;
    plot3(Ii(:,1),Ii(:,2),Ii(:,3),'b*')
text(xv,yv,zv,caption);
else if xx==0
    check=5;
    disp('no on the edge');
    end
end
end
all_plain_pts = [A;B;C;D];
if Wa==hitwall
```

```
    p=fill3(all_plain_pts(:,1),all_plain_pts(:,2),all_plain_pts(:,3),'black');
   alpha(0);
else
    p=fill3(all_plain_pts(:,1),all_plain_pts(:,2),all_plain_pts(:,3),'yellow');
    alpha(0);
end
    hold on
    all_line = [P1;Q1];
    plot3(all_line(:,1),all_line(:,2),all_line(:,3),'blue')
   xlabel('X')
    ylabel('Y')
   zlabel('Z')
   end

if xxx >= 1
    MaxSizeIntersected=max(size(ontheedge));
for j=1:MaxSizeIntersected;   % how many walls intersected
Intersected= ontheedge(j);  %stored the name of wall
Inter=char(Intersected);     % converted the name to character
DD=extractAfter(Inter,"Wall_");  %extracted the wall number from Inter
EE=str2num(DD);                    % converted to number
EEE(j)=EE;                    % all values of EE iteration are stored
FF=EEE ~=0;                     % removed zero location
E4=EEE(FF);
E5=fliplr(E4)
% all the wall number values except zero
end
mm=1;
for k=E4
A_2D=[xv2(k) yv2(k) zv2(k)];
distance_rx=norm(Q1-A_2D);
Distance_Rx(k)=distance_rx;
%mm=mm+1;
GG=Distance_Rx ~=0;
final_intersected_distance=Distance_Rx(GG);
Sorted_final_distance=sort(final_intersected_distance);
Sorted_final_distance_TX=fliplr(Sorted_final_distance);
AA1=wall(k).position(1,1:3);
BB2=wall(k).position(2,1:3);
CC=wall(k).position(3,1:3);
DD=wall(k).position(4,1:3);
end
sum=0
sizesortdist=max(size(Sorted_final_distance));
for m=1:sizesortdist
AA=Sorted_final_distance(m);
BB=find(AA);
II=find(final_intersected_distance==AA);
III=II(1);
JJ=E4(III);
Wall_closest_from_RX(m)=JJ;
Wall_closest_from_TX=fliplr(Wall_closest_from_RX);
end
view(2)
```

```
Intersected_walls;
ontheedge;
Wall_closest_from_RX;
Wall_closest_from_TX;
Lwx=[0:1:30];
Sum1=0;
for n=1:MaxSizeIntersected
    l=Wall_closest_from_RX(n);
    Typeofwall=wall(l).material
    if Typeofwall== "wood"
lossofwall=4;
elseif Typeofwall=="brick"
lossofwall=10;
else Typeofwall="glass"
lossofwall=3;
    end
    lk=lossofwall;
ll(n)=lk;
if ll>30
ll(n)=30;
end
Val=Lwx(ll+1);
Sum1=Sum1+lk;
end

C=300000000;
Frequency = 50*(10^8) ;
f=5000;
Noofwalls = MaxSizeIntersected;

for n=1:MaxSizeIntersected+1
Sorted_final_distance_TX(MaxSizeIntersected+1)=0;
Distance_X=distance-Sorted_final_distance_TX(n);
Distance_XX(n)=Distance_X;
end
for n=1
Distance_F=Distance_XX(1)
Distance_FF(n)=Distance_F;
if Distance_FF(n)<=0.5
    Distance_FF(n)=0.5
end
end
for n=2:MaxSizeIntersected+1
Distance_F=Distance_XX(n)-Distance_XX(n-1);
Distance_FF(n)=Distance_F;
if Distance_FF(n)<=0.5
    Distance_FF(n)=0.5
end
end
Lwx2=-Lwx./10;
Lwx3=10.^(Lwx2);
Lwxx=Lwx3.^Noofwalls;
kx1=(C^2)/((Frequency^2)*4*3.14);
kx2=(683*0.00002116*3.14)/4;
```

```
FX=(kx2.*Lwxx)/kx1;
Alphax1=nthroot(FX,Noofwalls);
X1=1./Alphax1;
Minimumval=min(Alphax1);
Maximumval=max(Alphax1);
normalizedval1=(Alphax1-Minimumval)/(Maximumval-Minimumval);  %transparency value
normalizedval=1-normalizedval1;
for n=1:MaxSizeIntersected
nVal=normalizedval(Val(n)+1);
end
Total_Distance=distance;
T_FSPL_1=20*log10(Total_Distance)+20*log10(f)+32.45;
D1=[5:1:35];
D=D1/1000;
x12=log10(D);
T_FSPL1=20*x12+20*log10(f)+32.45;
T_FSPL3=-T_FSPL1./10;
T_FSPL=10.^(T_FSPL3);
MinimumvalFSPL=min(T_FSPL);
MaximumvalFSPL=max(T_FSPL);
normalizedvalFSPL1=(T_FSPL-MinimumvalFSPL)/(MaximumvalFSPL-MinimumvalFSPL);
ref=5;
f1=2400;
normalizedvalFSP=((D1/ref).^(-2))*((f/f1)^(-2))
normalizedvalFSPL=1-normalizedvalFSP;
if distance < 6
    normalizedvalFSPL=0
end
nnVal=1;
for n=1:MaxSizeIntersected
    if distance < 6
    Transp=normalizedvalFSPL;
else
Transp=normalizedvalFSPL(int8(distance)-4)
    end
nVal=normalizedval(Val(n)+1);
Sval(n)=nVal;
nnVal=nnVal*nVal;
end
Comptransp=Transp*nnVal;
rrr=MaxSizeIntersected+1;
Rimg= imread('plain.png');
for n=1:MaxSizeIntersected
g=Wall_closest_from_TX(n);
    Type=wall(g).position;
xxImage = [wall(g).position(2,1) wall(g).position(1,1); wall(g).position(2,1)
wall(g).position(1,1)];
yyImage = [wall(g).position(2,2) wall(g).position(2,2); wall(g).position(2,2)
wall(g).position(2,2)];
zzImage = [3 3; 0 0];
rr=surf(xxImage,yyImage,zzImage,...
   'CData',Rimg,...
    'FaceColor','texturemap');
 alpha(rr,Sval(rrr-n));
```

```
end
cap1 = sprintf('TX');
text(X_coordinate_tx,Y_coordinate_tx,Z_coordinate_tx,cap1)
cap2 = sprintf('RX');
text(Xr,Yr,1,cap2)

D1=distance;
D=D1/1000;
xFSPL_1=log10(D)
FSPL=20*x12+20*log10(f)+32.45;
Total_FSPL_Loss= FSPL
Intertran_FSPL1=Total_FSPL_Loss;
Intertran_Walls1=Sum1;
Comptransp1=Intertran_FSPL1+Intertran_Walls1;
else
    Total_Distance=distance;
    T_FSPL_1=20*log10(Total_Distance)+20*log10(f)+32.45;
D1=[5:1:35];
D=D1/1000;
x12=log10(D);
T_FSPL1=20*x12+20*log10(f)+32.45;
T_FSPL3=-T_FSPL1./10;
T_FSPL=10.^(T_FSPL3);
MinimumvalFSPL=min(T_FSPL);
MaximumvalFSPL=max(T_FSPL);
normalizedvalFSPL1=(T_FSPL-MinimumvalFSPL)/(MaximumvalFSPL-MinimumvalFSPL);
ref=5;
f1=2400;
normalizedvalFSP=((D1/ref).^(-2))*((f/f1)^(-2))
normalizedvalFSPL=1-normalizedvalFSP;
if distance < 6
    normalizedvalFSPL=0
end

D1=distance;
D=D1/1000;
xFSPL_1=log10(D)
FSPL=20*x12+20*log10(f)+32.45;
Total_FSPL_Loss= FSPL
Intertran_FSPL3=Total_FSPL_Loss;
Comptransp1=(Intertran_FSPL3);
SS=20-Comptransp1;
cap1 = sprintf('TX');
text(X_coordinate_tx,Y_coordinate_tx,Z_coordinate_tx,cap1)
cap2 = sprintf('RX');
text(Xr,Yr,1,cap2)
end
clearvars E4 final_intersected_distance Sorted_final_distance Distance_Rx ;
end
img = imread('exercise.jpg');
xImage = [Q1(1)-0.5 Q1(1)+0.5; Q1(1)-0.5 Q1(1)+0.5];
yImage = [Q1(2) Q1(2); Q1(2) Q1(2)];
zImage = [3 3; 0 0];
surf(xImage,yImage,zImage,...
```

```
   'CData',img,...
    'FaceColor','texturemap');
xxxImage = [P1(1)-0.5 P1(1)+0.5; P1(1)-0.5 P1(1)+0.5];
yyyImage = [P1(2) P1(2); P1(2) P1(2)];
zzzImage = [3 3; 0 0];
if distance < 6
    TranspF=normalizedvalFSPL;
else
TranspF=normalizedvalFSPL(int8(distance)-4)
end
Rimg= imread('plain.png');
rr4=surf(xxxImage,yyyImage,zzzImage,...
   'CData',Rimg,...
    'FaceColor','texturemap');
 alpha(rr4,TranspF);
axis([0 2 0 8 0 3])
clc
view(3)
view(11,25)
clc
P1
Q1
distance
```

REFERENCES

[1] D. Cichon, T. Kürner, and T. Research-Action, "Digital mobile radio towards future generation systems: Cost 231 final report," vol. 231, 1993

[2] J. Walfisch, H. Bertoni, and propagation, "A theoretical model of UHF propagation in urban environments," vol. 36, no. 12, pp. 1788-1796, 1988.

[3] R. Cruz, F. da Costa, P. Braga, G. Fontgalland, M. B. de Melo, and R. Do Valle, "A comparison between theoretical propagation models and measurement data to distinguish urban, suburban and open areas in Jodo Pessoa, Brazil," in *Microwave and Optoelectronics, 2005 SBMO/IEEE MTT-S International Conference on*, 2005, pp. 287-291: IEEE.

[4] T. Sarkar, Z. Ji, K. Kim, A. Medouri, M. Salazar-Palma, and p. Magazine, "A survey of various propagation models for mobile communication," vol. 45, no. 3, pp. 51-82, 2003.

[5] M. F. Iskander, Z. Yun, and techniques, "Propagation prediction models for wireless communication systems," vol. 50, no. 3, pp. 662-673, 2002.

[6] S. Zvanovec, M. Valek, and P. Pechac, "Results of indoor propagation measurement campaign for WLAN systems operating in 2.4 GHz ISM band," 2003.

[7] T. Rappaport, "Wireless Communications--Principles and Practice, (The Book End)," vol. 45, no. 12, pp. 128-129, 2002.

[8] A. Motley and J. J. E. L. Keenan, "Personal communication radio coverage in buildings at 900 MHz and 1700 MHz," vol. 24, no. 12, pp. 763-764, 1988.

[9] M. Lott and I. Forkel, "A multi-wall-and-floor model for indoor radio propagation," in *Vehicular Technology Conference, 2001. VTC 2001 Spring. IEEE VTS 53rd*, 2001, vol. 1, pp. 464-468: IEEE.

[10] H. Suzuki, "A statistical model for urban radio propogation," vol. 25, no. 7, pp. 673-680, 1977.

[11] F. Babich and G. Lombardi, "Statistical analysis and characterization of the indoor propagation channel," vol. 48, no. 3, pp. 455-464, 2000.

[12] A. A. Saleh and R. Valenzuela, "A statistical model for indoor multipath propagation," vol. 5, no. 2, pp. 128-137, 1987.

[13] H. Hashemi, "Impulse response modeling of indoor radio propagation channels," vol. 11, no. 7, pp. 967-978, 1993.

[14] K.-W. Cheung, J.-M. Sau, and R. Murch, "A new empirical model for indoor propagation prediction," vol. 47, no. 3, pp. 996-1001, 1998.

[15] R. Akl, D. Tummala, and X. Li, "Indoor Propagation Modeling at 2.4 GHz for IEEE 802.11 Networks," in *Wireless and Optical Communications*, 2006.

[16] A. Bhuvaneshwari, R. Hemalatha, and T. Satyasavithri, "Semi Deterministic Hybrid Model for Path Loss Prediction Improvement," vol. 92, pp. 336-344, 2016.

[17] J. Shaw, "Radiometry and the Friis transmission equation," vol. 81, no. 1, pp. 33-37, 2013.

[18] D.-T. Phan-Huy *et al.*, "The Radio Waves Display: an Intuitive Way to Show Green Techniques for 5G to the General Public," in *2017 IEEE International Conference on Communications Workshops (ICC Workshops)*, 2017, pp. 234-240: IEEE.

[19] S. Mann, "Phenomenal Augmented Reality: Advancing technology for the future of humanity," vol. 4, no. 4, pp. 92-97, 2015.

[20] P. Scourboutakos, M. H. Lu, S. Nerker, and S. Mann, "Phenomenologically augmented reality with new wearable led sequential wave imprinting machines," in *Proceedings of the Eleventh International Conference on Tangible, Embedded, and Embodied Interaction*, 2017, pp. 751-755: ACM.

[21] P. Scourboutakos, "New Sequential Wave Imprinting Machines Visualize Waves in Real-space and Real-time by Augmediating Reality," 2016.

[22] S. Mann, T. Furness, Y. Yuan, J. Iorio, and Z. J. a. p. a. Wang, "All Reality: Virtual, Augmented, Mixed (X), Mediated (X, Y), and Multimediated Reality," 2018.

[23] R. Azuma and V. Environments, "A survey of augmented reality," vol. 6, no. 4, pp. 355-385, 1997.

[24] W. Mann, "Eye-tap for electronic newsgathering, documentary video, photojournalism, and personal safety," ed: Google Patents, 2003.

[25] D. McMillen, "Spatial autocorrelation or model misspecification?," vol. 26, no. 2, pp. 208-217, 2003.

[26] A. Katiyar, K. Kalra, C. J. A. i. C. S. Garg, and I. Technology, "Marker based augmented reality," vol. 2, no. 5, pp. 441-445, 2015.

[27] A. I. Comport, É. Marchand, and F. Chaumette, "A real-time tracker for markerless augmented reality," in *Proceedings of the 2nd IEEE/ACM International Symposium on Mixed and Augmented Reality*, 2003, p. 36: IEEE Computer Society.

[28] A. Cebulla, "Projection-based augmented reality," 2013.

[29] S. Feiner, "Augmented reality: A new way of seeing," vol. 286, no. 4, pp. 48-55, 2002.

[30] A. Al-Alawi, "WiFi technology: Future market challenges and opportunities," vol. 2, no. 1, pp. 13-18, 2006.

[31] Metageek.com. (2018). *Dead Spots and Slow Zones*. Available: https://www.metageek.com/training/resources/dead-spots-slow-zones

[32] D. M. Leive, "International Telecommunications and International Law: The Regulation of the Radio Spectrum," 1970.

[33] G. Koutitas, "RF Propagation and Antenna Theory," Texas State University, 2016.

[34] J. Shirley, "An early experimental determination of Snell's law," vol. 19, no. 9, pp. 507-508, 1951.

[35] W. Tam, V. J. E. Tran, and C. E. Journal, "Propagation modelling for indoor wireless communication," vol. 7, no. 5, pp. 221-228, 1995.

[36] R. Rudd, K. Craig, M. Ganley, and R. J. F. R. Hartless, Ofcom, "Building materials and propagation," vol. 2604, 2014.

[37] A. Sohail, Z. Ahmad, I. Ali, and Technology, "Analysis and measurement of Wi-Fi signals in indoor environment," vol. 6, no. 2, p. 678, 2013.

[38] W. L. Stutzman and G. A. Thiele, *Antenna theory and design*. John Wiley & Sons, 2013.

[39] Y. Bultitude and T. Rautiainen, TUI, UOULU, CU/CRC, NOKIA, Tech. Rep., Tech. Rep, "IST-4-027756 WINNER II D1. 1.2 V1. 2 WINNER II Channel Models," 2007.

[40] A. Zyoud, J. Chebil, M. H. Habaebi, M. R. Islam, and A. M. Zeki, "Comparison of empirical indoor propagation models for 4G wireless networks at 2.6 GHz," in *Proceedings Engineering & Technology*, 2013, vol. 3, pp. 7-11.

[41] W. Dong, J. Zhang, X. Gao, P. Zhang, and Y. Wu, "Cluster identification and properties of outdoor wideband MIMO channel," in *Vehicular Technology Conference, 2007. VTC-2007 Fall. 2007 IEEE 66th*, 2007, pp. 829-833: IEEE.

[42] T. f.-. Fujii, ” Trans. IEICE, Japan, J86-B, "Path loss prediction formula in mobile communication-an expansion of," vol. 10, pp. 2264-2267, 2003.

[43] Y. Lu, J. Zhang, X. Gao, P. Zhang, and Y. Wu, "Outdoor-indoor propagation characteristics of peer-to-peer system at 5.25 GHz," in *Vehicular Technology Conference, 2007. VTC-2007 Fall. 2007 IEEE 66th*, 2007, pp. 869-873: IEEE.

[44] D. Xu, J. Zhang, X. Gao, P. Zhang, and Y. Wu, "Indoor office propagation measurements and path loss models at 5.25 GHz," in *Vehicular Technology Conference, 2007. VTC-2007 Fall. 2007 IEEE 66th*, 2007, pp. 844-848: IEEE.

[45] J. Zhang, X. Gao, P. Zhang, and X. Yin, "Propagation characteristics of wideband MIMO channel in hotspot areas at 5.25 GHZ," in *Personal, Indoor and Mobile Radio Communications, 2007. PIMRC 2007. IEEE 18th International Symposium on*, 2007, pp. 1-5: IEEE.

[46] J. Zhang *et al.*, "Propagation characteristics of wideband MIMO channel in urban micro-and macrocells," in *Personal, Indoor and Mobile Radio Communications, 2008. PIMRC 2008. IEEE 19th International Symposium on*, 2008, pp. 1-6: IEEE.

[47] V. R. Jewell, "Use of GIS in Radio Frequency and Positioning Applications," Virginia Tech, 2014.

[48] W. R. McCluney, *Introduction to radiometry and photometry*. Artech House, 2014.

[49] I. Ashdown and P. Eng, "Photometry and radiometry," 2002.

[50] P. D. Hiscocks and P. Eng, "Measuring luminance with a digital camera," vol. 16, 2011.

[51] E. F. Schubert, *Light-emitting diodes*. E. Fred Schubert, 2018.

[52] O. Gal and R. Chen-Morris, "The archaeology of the inverse square law:(1) Metaphysical images and mathematical practices," vol. 43, no. 4, pp. 391-414, 2005.

[53] R. Abdelrahman, A. Mustafa, and A. A. Osman, "A Comparison between IEEE 802.11 n and ac Standards," 2015.

[54] J. o'Rourke, *Computational geometry in C*. Cambridge university press, 1998.